

The Kinetics of Myeloid Derived Suppressor Cell Frequency and Function in Chronic
Retroviral Infections

Sandra Dross

A dissertation
submitted in partial fulfillment of the
requirements for the degree of

Doctor of Philosophy

University of Washington

2016

Reading Committee:

Dr. Helen Horton, Chair

Dr. Jennifer Friesen

Dr. Kevin Urdahl

Program Authorized to Offer Degree:

Pathobiology

©Copyright 2016
Sandra Dross

University of Washington

Abstract

The Kinetics of Myeloid Derived Suppressor Cell Frequency and Function in Chronic Retroviral Infections

Sandra Dross

Chair of the Supervisory Committee:

Helen Horton, PhD.

Department of Medicine and Public Health

During chronic retroviral infection, poor clinical outcomes correlate both with systemic inflammation and poor proliferative ability of HIV-specific T cells, however the connection between the two is not clear. Myeloid derived suppressor cells (MDSC), suppressive cells of myeloid origin that accumulate during states of elevated circulating inflammatory cytokines, may link the systemic inflammation and poor T cell function characteristic of retroviral infections. MDSC have been partially characterized in retroviral infections, and questions remain regarding their phenotype, persistence, activity and clinical significance in HIV and SIV infection. We enrolled HIV+ individuals on combination antiretroviral therapy (cART) across a spectrum of ages and found significantly elevated frequencies of MDSC of granulocytic (gMDSC) and not monocytic (mMDSC) origin in HIV+ individuals over the age of 50 compared to age-matched HIV-

individuals. These gMDSC suppressed *ex vivo* HIV-specific T cell responses. We then followed rhesus macaques (*Macaca mulatta*) over the course of SIV infection. We observed low frequencies of MDSCs pre-SIV infection and elevated gMDSC at all stages of SIV infection that increased most markedly at 20 weeks post-cART. These cells exert suppressive effects on T cell responses to polyclonal and SIV peptide stimuli. In both models MDSC frequency correlated with levels of circulating inflammatory cytokines. In the animal model the cytokines independently correlating with MDSC were characteristic of microbial translocation. While MDSC have been previously described in HIV and SIV infection, novel findings of this work are the two distinct times of elevated inflammation in chronic retroviral infection leading to accumulation of MDSC. MDSC are elevated during aging even in a cART-suppressed host, and MDSC are markedly elevated during treatment interruption in a previously cART-suppressed host. This work highlights a potential risk of non-adherence, or treatment interruption, in cART-suppressed HIV+ individuals. This is important because the US Department of Health and Human Services recommend all HIV+ individuals initiate antiretroviral therapy regardless of CD4 count. Future work exploring therapies to abrogate microbial translocation or disable MDSC suppression at these times in retroviral infection may be warranted.

Table of Contents

Abstract.....	3
List of figures.....	7
Chapter 1: Introduction.....	8
1.0 Myeloid-derived suppressor cells	8
1.1 MDSC suppressive mechanisms	9
Depletion of amino acids in the microenvironment	10
Interference with T cell homing and viability.....	11
Generation of oxidative stress	11
Indirect suppression by MDSC via the generation of T-regulatory cells	11
1.2 MDSC in chronic viral infections	12
Hepatitis B Virus (HBV).....	12
Hepatitis C Virus (HCV)	13
HIV	14
SIV	15
1.3 Immune response to retroviral infection.....	16
1.4 Aims and hypotheses	17
Chapter 2: MDSC in HIV+ aging individuals on suppressive antiretroviral therapy	20
2.0 Introduction	20
2.1 gMDSC frequency is elevated in older HIV+ men on antiretroviral therapy	22
2.2 gMDSC suppress HIV Gag-specific responses.....	28
2.3 gMDSC require contact or proximity to exert suppressive effects	28
2.4 Inflammatory cytokines correlate with gMDSC levels.....	32
2.5 Discussion	34
Chapter 3: Kinetics of myeloid derived suppressor cell frequency and function during SIV infection, combination antiretroviral therapy and treatment interruption.....	38
3.0 Introduction	38
3.1 MDSC frequency is elevated at all stages of SIV infection	40
3.2 MDSC suppress SIV-specific and polyclonally stimulated T cell responses.....	48
3.3 MDSC in lymphoid tissue exhibit suppressive function	50
3.4 Plasma cytokine levels correlate with MDSC	50
3.5 MDSC frequency pre-SIV correlates with set-point viral load.....	55
3.6 MDSC are not induced in culture by SIV.....	55

3.7 Soluble CD14 levels elevated post-cART	56
3.8 Discussion of MDSC kinetics during SIV infection	60
Chapter 4: Final discussion	64
4.0 Discussion	64
4.1 Summary	67
4.2 Further questions	70
4.3 Concluding statement and implications	73
Methods	74
Cross-sectional MDSC characterization in HIV infection	74
Specimen collection	74
MDSC frequency determination	74
MDSC depletion and functional experiments	74
Mechanistic experiments	75
Contact dependence	76
Cytokine analyses	76
Density separation method testing	76
Longitudinal MDSC kinetics in SIV-infection methods	77
Specimen collection	77
Blood processing	77
Staining	78
MDSC isolation and PBMC co-cultures	78
Tissue processing at necropsy	79
Plasma Cytokine Levels	79
Induction of MDSC via SIV viral products	80
Statistical Analyses	80
Appendix A: Experimental optimization prior to longitudinal MDSC analyses	81
Acknowledgements	84
Vita	85
References	86

List of figures

Figure 1. Visual representation of hypothesis.....	19
Table 1. Population demographics.....	24
Figure 2. MDSC gating strategy and representative plots.....	25
Figure 3. Women have higher MDSC frequencies than men.....	26
Figure 4. MDSC frequency is elevated in older HIV+ vs. HIV- men.....	27
Figure 5. MDSC suppress HIV Gag, but not CMV or polyclonal, stimulated T cell proliferation.....	30
Figure 6. Transwell® abrogates MDSC suppressive function while arginine rescue has no effect.....	31
Figure 7. MDSC levels correlate with MDSC-expanding cytokines.....	33
Figure 8. Study design and MDSC gating strategy.....	43
Figure 9. Myeloid-Derived Suppressor Cell Frequency in Chronic SIV infection: Pilot study.....	44
Figure 10. Myeloid-Derived Suppressor Cell Frequency in Chronic SIV infection: Longitudinal Study.....	45
Figure 11. Individual Viral load, MDSC Frequency and CD4 Kinetics.....	46
Figure 12. MDSC frequency of cells correlates tightly with cells/ul blood.....	47
Figure 13. gMDSC suppress T cell proliferation at all stages of infection.....	49
Figure 14. MDSC frequency in peripheral lymphoid organs.....	52
Table 2. Plasma cytokine levels correlated with MDSC frequency.....	53
Figure 15. Plasma cytokine levels over course of SIV infection.....	54
Figure 16. MDSC frequency pre-infection correlates with higher viral loads.....	57
Figure 17. SIV does not induce MDSC in culture.....	58
Figure 18. Levels of sCD14 elevated during post-cART viremia.....	59
Figure 19. Model of MDSC in retroviral infection.....	69

Chapter 1: Introduction

1.0 Myeloid-derived suppressor cells

Myeloid-derived suppressor cells (MDSC) are a heterogeneous group of immunosuppressive cells of myeloid origin. MDSC were originally described, and have canonically been characterized, in mouse tumor models and cancer patients where they inhibit natural anti-tumor responses and correlate with poor outcomes (reviewed in [1]). When MDSC are ablated, either natural immunity or chemotherapeutic agents have been found to be more efficacious. In healthy individuals MDSC are infrequent as they differentiate into macrophages, dendritic cells or neutrophils upon exiting the bone marrow into the periphery.

During chronic states of elevated inflammation immature myeloid cells enter the periphery and do not fully differentiate into lineage-committed cells. It is thought that activation prior to differentiation results in suppressive function and this may be the factor that hinders differentiation [2]. Signal transducer and activator of transcription 3 (STAT3) is the major transcription factor responsible for accumulation and activation of MDSC. STAT3 up-regulates factors important for cell survival and suppressive function while down-regulating key molecules important for myeloid cell differentiation, thereby blocking full lineage commitment. Pro-inflammatory cytokines that signal through STAT3 and are implicated in MDSC expansion and activation include IL-1 β , IL-6, G-CSF, GM-CSF, and VEGF [1].

In the absence of cancer or chronic infection MDSC play a poorly characterized role during trauma and wound healing. MDSC in these contexts are thought to assist in

dampening immune responses to reduce development of self-reactivity and also promote blood vessel formation [3]. These functions are co-opted in a cancerous host where MDSC are recruited by tumor-secreted factors, facilitate angiogenesis and dampen anti-cancer immune responses [4].

The term ‘myeloid-derived suppressor cell’ is relatively new as it was first mentioned in the literature in 2005. Cells of similar phenotype and function were described as myeloid-suppressor cells (MSC) starting in 2000, and null cells, veto cells or natural suppressor (NS) cells in the mid-1900s (reviewed in [5]). MDSC methods of identification have had a similar evolutionary trajectory as the nomenclature of such cells, and there is a wide range of surface markers utilized to characterize these cells. In summary, the basic hallmark of an MDSC-identifying panel in humans is one that can identify cells of myeloid origin (for humans, utilizing the myeloid marker CD11b or CD33) that are not functionally mature (Lack of HLA-DR). In addition, many (but not all) groups characterize whether the MDSC are granulocytic (gMDSC, identified by granulocyte marker CD15+ or CD66+) or monocytic (mMDSC, identified by monocyte marker CD14+).

1.1 MDSC suppressive mechanisms

MDSC suppress T cell function directly by three main classes of mechanisms: depletion of necessary amino acids in the microenvironment, interaction with T cell surface molecules important for homing and viability, and generation of reactive nitrogen and oxygen species. MDSC can additionally suppress T cell function indirectly through the induction of T regulatory cells (reviewed in [1]). MDSC also skew innate immune

function towards alternative phenotypes (M2 macrophage skewing, NK cell dysfunction) to promote tumor progression (reviewed in [6]); however, the majority of the literature focuses on T cell suppression, discussed below.

Depletion of amino acids in the microenvironment

MDSC express arginase-1 which acts to deplete arginine in the microenvironment. Arginine is necessary for expression of the TCR ζ chain, which contains the majority of ITAMs necessary for TCR signaling [7]. Arginine depletion by MDSC-secreted arginase-1 in the microenvironment abrogates TCR signaling and T cell responses to stimulus by TCR CD3 ζ -chain downregulation [8]. Depletion of arginine in the microenvironment also causes T cells to arrest in G0-G1 phase [9]. Arginase-1 is expressed by both monocytic and granulocytic subsets of MDSC in mice while arginase-1 expression is limited to granulocytes in humans and, therefore, is not thought to be expressed in human mMDSC [10].

Cysteine sequestration is another mechanism by which MDSC are thought to suppress T cells via depletion of essential amino acids from the microenvironment. Cysteine is an amino acid necessary for proliferation and protein generation in all cells, but T cells lack the ability to import and convert cystine to cysteine and also cannot metabolize methionine to cysteine. Therefore, T cells depend on antigen presenting cells (APCs) to provide cysteine, which serves as another regulatory ‘co-stimulation’ step in the immune response to avoid unwanted T cell responses [6]. T cell suppression via importation and sequestration of cysteine by MDSC has been observed in a mouse model. This effect was partially rescued by increasing cysteine levels in culture. Furthermore,

animals with tumors had significantly lower levels of cystine than animals without, suggesting sequestration of cysteine plays a role in MDSC function [11].

Interference with T cell homing and viability

MDSC impair T cell homing by cell surface expression of disintegrin and metalloproteinase-containing protein 17 (ADAM17) which cleaves L-selectin (CD62L) from the surface of naïve T cells. In the absence of CD62L, naïve T cells cannot home to peripheral lymphoid organs and, therefore, are not primed [6]. MDSC also express cell surface galectin-9 which induces apoptosis upon binding to Tim-3 expressed on activated or exhausted T cells [12]. Additionally, MDSC in the tumor environment have been found to express PD-L1. PD-1 is upregulated on both activated and exhausted T cells. Signaling through PD-1 on T cells by interaction with PD-L1 reduces T cell functionality including proliferation, cytokine secretion and CD8-mediated killing [13]. Abrogation of PD-1/PD-L1 interaction improves cancer outcomes in humans [14].

Generation of oxidative stress

When produced by MDSC, the reactive oxygen species (ROS) and reactive nitrogen species (NOS) peroxynitrite, nitric oxide and hydrogen peroxide negatively affect T cell: APC interactions and T cell signaling. The T-cell receptor (TCR), as well as CD3 and CD8, can be nitrosylated and nitrated to reduce MHC binding. ROS and NOS can also decrease TCR ζ chain surface expression, reducing T cell signaling [15].

Indirect suppression by MDSC via the generation of T-regulatory cells

gMDSC in mice have been shown to secrete IL-10 which can both suppress T cell function directly and indirectly via the generation of T-regulatory cells. In humans it is not thought that granulocytes secrete IL-10, relegating this mechanism to mouse gMDSC

alone [16]. Recently, however, IL-10 secretion has been observed in granulocytes of human melanoma patients driven by increased serum amyloid A-1 (SAA-1) levels [17]. In these patients IL-10 producing granulocytes directly suppressed antigen-stimulated T-cell proliferation. While circulating SAA levels have been found to be elevated during both acute and chronic viral infections including rhinovirus, influenza and HIV infection [18, 19], they are on average higher in acute infections and in the early stages of chronic infections [20, 21] including HIV [22, 23]. Also, studies indicate SAA levels remain relatively stable during the aging process [24, 25]. These findings indicate SAA flux is not likely driving differential IL-10 production by granulocytic MDSC in our aging and chronically HIV+ populations.

1.2 MDSC in chronic viral infections

MDSC are elevated and immunosuppressive during chronic viral infections including, but not limited to, retroviral infections. Elevation of suppressive MDSC during chronic hepatitis C (HCV) infection is well characterized (reviewed in [26]). Elevated frequencies of MDSC have been recently reported in the livers of hepatitis B virus (HBV) positive mice [27]. In the LCMV model, study of acute and chronic forms of the same virus indicate MDSC are induced by chronic infection but not acute infection [28]. The majority of MDSC induction is described in chronic, not acute, infections in humans, discussed below.

Hepatitis B Virus (HBV)

Elevation of mMDSC with contact-independent CD8-T cell suppression has been observed in chronic HBV infection [29]. The majority (>75%) of these individuals were

diagnosed as 'immune-active', presenting with elevated liver inflammation and serum enzymes while the remainder were immune-tolerant carriers, with HBV viral replication but little liver inflammation and normal serum liver enzymes. The majority of these individuals were relatively young (average age 30) and male (~70%). Counter-intuitively, the mMDSC population was not different between immune-tolerant and immune-active groups nor concomitantly with progressing liver disease grade or stage. Evidence suggested IL-10 secretion was the suppressive mechanism of these mMDSC.

Hepatitis C Virus (HCV)

Elevation of MDSC have been observed in HCV-infected individuals vs. healthy controls which decrease after 4 weeks of effective PEG-IFN + ribavirin [30]. The subset defined was non-monocytic (but no granulocytic marker was used) and these MDSC were elevated in chronically infected, treatment-naïve individuals. MDSC frequency correlated directly with the circulating HCV RNA viral load and indirectly with the TCR ζ expression on autologous CD8 T cells. During IFN treatment, TCR ζ expression increased while MDSC frequency, serum alanine transaminase (ALT) and HCV RNA all decreased [31]. However, there is not complete agreement in regards to MDSC frequency and function over the course of HCV infection. Nonnenmann et al. found that HCV+ individuals did not have significantly elevated circulating gMDSC nor mMDSC frequencies while a positive-control group of viremic HIV+ individuals did have significant elevation of gMDSC [32]. They found no correlations between HCV viral load and gMDSC nor mMDSC frequency, and no significant differences in frequency when grouped by liver pathology stage. This group also determined that gMDSC had equivalent suppressive function (suppressing CD8 T cell proliferation and IFN γ

production) in healthy controls compared to the HCV+ individuals. Nonnenmann et al. have suggested that differences between their work and the previous published work can be attributed to the use of frozen PBMC in the prior studies, as it has been determined that gMDSC frequency and function can only be accurately measured in fresh cells [33, 34].

HIV

Six separate studies have shown elevated MDSC frequency in HIV infection [35-40]. MDSC frequency has been correlated with viral load and decreased numbers have been demonstrated with viral suppression. Negative correlations between CD4 count and MDSC frequency have also been reported. However, there is a fair amount of discrepancy regarding which subset, granulocytic or monocytic, is playing the suppressive role in infection. Three groups reported increased frequencies of gMDSC in HIV+ individuals [35, 36, 39] whereas three groups reported increased frequency of mMDSC [37, 38, 40]. Frequency of mMDSC correlated with increasing viral load, decreasing CD4 count, increasing % CD8 activation and advanced HIV clinical stage and suppressed both CD4 and CD8 T cell proliferation [37, 38, 40].

In HIV infection both gMDSC and mMDSC suppress T cells, but different mechanisms have been implicated in these studies. Vollbrecht et al. reported that gMDSC suppressed CD8 T cell proliferation when comparing PBMC to gMDSC-depleted PBMC. These gMDSC expressed IL4R α (CD124), and the authors suggested this may help differentiate suppressive vs. non suppressive MDSC. Bowers et al. reported correlations with gMDSC expression of programmed death-ligand 1 (PD-L1), in relation to programmed cell death protein-1 (PD-1), receptor expression on both CD4 and CD8

cells. They proposed MDSC PD-L1 signaling through PD-1 on CD4 and CD8 T cells is suppressing T cell function. Finally, Tumino et al. demonstrated that gMDSC induce T cell anergy by suppressing expression of CD3 ζ expression on T cells. For the studies reporting suppressive mMDSC, Qin et al. observed CD4 and CD8 suppression by MDSC that had elevations in expression of arginase-1. Garg et al. reported that mMDSC induced by HIV reduced IFN γ secretion upon co-culture with T cells; however, they did not report mechanism of suppression.

SIV

MDSC or MDSC-like populations in SIV infection have been characterized by two groups to date. Gama et al. described a population of monocytes with altered CCR2 surface expression, impaired inflammatory cytokine production, phagocytosis and chemotaxis, and the ability to suppress CD8 T cell proliferation in a pigtailed macaque (*Macaca nemestrina*) SIV infection model [41]. These cells decreased in frequency during antiretroviral therapy to levels comparable to SIV-free controls. Sui et al. described two populations of MDSC, total and monocytic, that increased in frequency post-vaccination in animals receiving SIV vaccine compared to animals receiving adjuvant alone [42]. These MDSC suppressed CD8 proliferative responses to SIV in a dose-dependent manner. In animals receiving the SIV vaccine, set-point viral load positively correlated with the frequency of peripheral mMDSC and total MDSC, and frequency of the colorectal tissue mMDSC alone. The adjuvant-only animals in this study displayed better virologic control and no less protection from infection compared to the vaccinated group, suggesting MDSC were elicited by viral peptides and hampered immune control of SIV.

1.3 Immune response to retroviral infection

During pathogenic retroviral infections including HIV and SIV, cellular and humoral immune responses are insufficient to clear acute infection, leading to disease progression for most individuals. In these individuals, despite initial effective cellular responses critical for viral control, T cells lose functional capacity leading to disease progression [43]. A small subset of individuals called HIV controllers maintain T cell polyfunctionality and proliferative ability, retaining the ability to control viral replication and disease progression in the absence of antiretroviral therapy. Of T cell functions, loss of proliferative ability in response to HIV-stimulation is the strongest independent predictor of progression vs. control [44].

Inflammation during acute infection serves to drive and tune the innate and adaptive immune responses. In retroviral infection, this inflammation persists as these responses are insufficient to resolve viral replication and the latent reservoir is established. Systemic inflammation is a hallmark of chronic pathogenic retroviral infections and contributes greatly to the immune dysfunction observed. In retroviral infection chronic systemic inflammation is induced by viral replication and microbial translocation and is dampened but persists during virologic suppression [45, 46]. Indeed, immune activation correlates stronger with poor prognosis than viral load or co-receptor use alone [47].

The causes of T cell dysfunction in progressive retroviral infection and the link between cellular dysfunction and immune-activation dependent disease outcomes are not yet completely understood. MDSC are expanded and activated in the pro-inflammatory

environment typical of retroviral infection, and it is likely that they contribute to this immune dysfunction.

1.4 Aims and hypotheses

Our primary aim was to determine the role MDSC play in the cellular dysfunction associated with chronic retroviral infection in a virally-suppressed, aging host. It has been well described that even in the absence of viral replication HIV+ individuals respond poorly to vaccines and develop age-associated morbidities such as heart disease and cancer earlier and/or more frequently than their age-matched HIV- peers [48]. We suspected that MDSC induced by HIV infection *and* aging may be playing a role in the dwindling immune responses in this population. Elevated MDSC frequencies have been described separately in both the elderly [49] and HIV+ populations [35, 37-40] but had not yet been characterized in the aging HIV+ population. In addition, the majority of publications describing MDSC in HIV infection focused on virally unsuppressed or recently suppressed populations. In our studies, we focused on an as-yet-uncharacterized population, but one that is growing: those who have been HIV+ for at least five years and virally suppressed for at least one year, and many individuals over the age of 50.

We hypothesized that T cell suppression plays a role in the observed immune dysfunction associated with chronic HIV infection and aging, as MDSC accumulate as a result of prolonged inflammation—a hallmark of both HIV-infection and aging. Additionally, we hypothesized that during normal aging the increased pro-inflammatory environment drives the accumulation of MDSC, but that this accumulation was accelerated and amplified in age-matched HIV+ individuals. Furthermore, we

hypothesized that MDSC participate in the impairment of T cell proliferation, homeostasis and response to antigen.

Our secondary aim was to delineate the kinetics of MDSC frequency and function in retroviral infection. Due to the difficulty in probing the early stages of HIV infection in humans, we turned to an animal model. Pathogenic retroviral infection in a Rhesus macaque model recapitulates the immune dysfunction observed in HIV infection in humans. We focused on assaying MDSC frequency and function in uninfected rhesus macaques for a baseline measure, then characterized MDSC frequency and function over the course of SIV infection including during acute infection, combination antiretroviral therapy (cART) treatment and post-treatment interruption.

For our secondary aim we hypothesized MDSC would be infrequent in healthy rhesus macaques and elevated in acute SIV infection. We hypothesized this population would wane during chronic cART treatment and emerge post treatment interruption at levels similar or greater to those observed during acute infection. Lastly, we hypothesized these MDSC would suppress SIV responses.

Combining these aims, our overarching hypothesis is that MDSC are induced by the inflammation characteristic of chronic retroviral infection, and that these MDSC contribute to the decreased T cell function observed over the course of infection (Figure 1).

Hypothesis

MDSC induced by inflammation in chronic retroviral infections contribute to the decreased T cell function observed over the course of infection

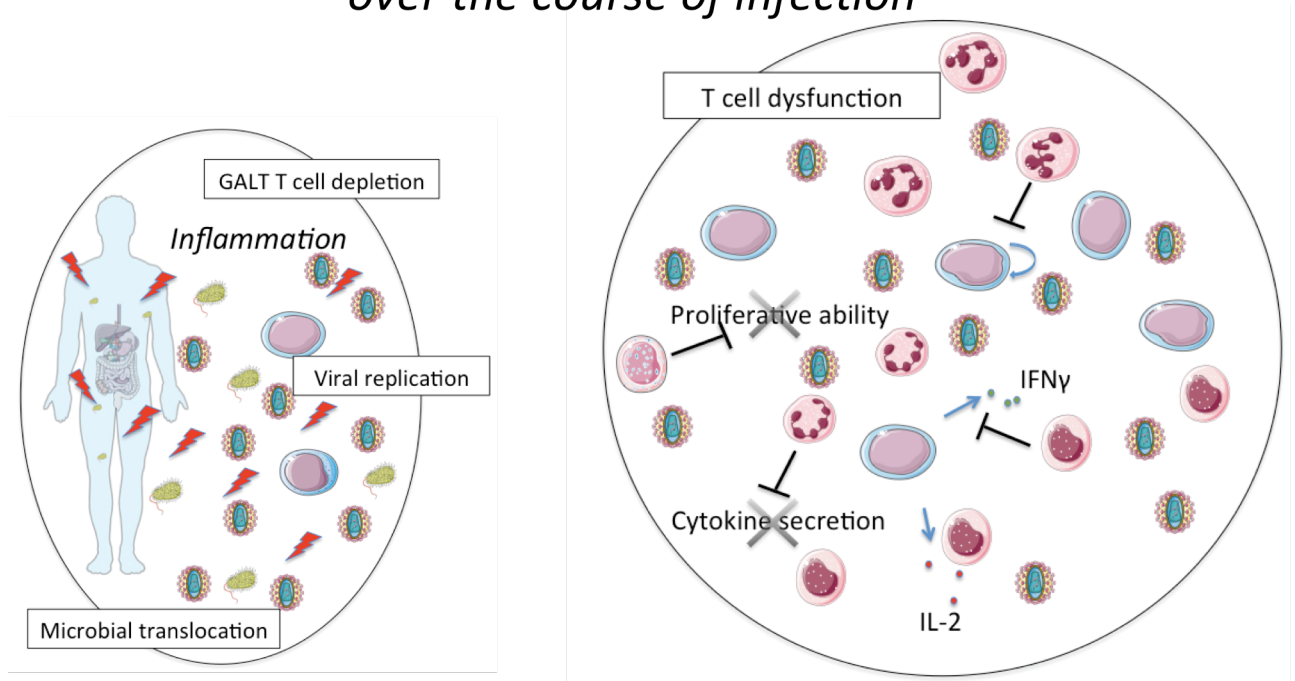


Figure 1. Visual representation of hypothesis

During chronic retroviral infection poor clinical outcomes correlate both with systemic inflammation and poor proliferative ability of HIV-specific T cells; however, the connection between the two is not clear. During retroviral infection, inflammation is driven by immune responses to viral replication and microbial translocation. This activation and T cell dysfunction persists even after viral replication is abrogated by antiretroviral therapy. Myeloid derived suppressor cells (MDSC), suppressive cells of myeloid origin that expand during states of elevated circulating inflammatory cytokines, may link the systemic inflammation and poor T cell function characteristic of retroviral infections. We hypothesize that MDSC are induced by the inflammation characteristic of chronic retroviral infection, and that these MDSC contribute to the decreased T cell function observed over the course of infection.

Chapter 2: MDSC in HIV+ aging individuals on suppressive antiretroviral therapy

2.0 Introduction

The elderly and aging HIV+ populations are expanding rapidly in the US and worldwide [50-53]. In fact, according to the WHO, the proportion of aging individuals is expanding faster than any other age group in almost every country in the world. In the US, an estimated 20% of the general population will be 65+ by 2050 and an estimated half of HIV+ individuals are 50+ years old today [50, 51]. The aging of the HIV+ population is a triumph of research and medicine as the life expectancies of HIV+ individuals move closer to that of HIV- individuals [54]. This phenomenon now extends beyond the developed world as ART becomes more available and more affordable worldwide [55]. Chronic HIV infection and aging are independently associated with poor responses to vaccines and infection [56-60]. It is necessary to gain a better understanding of why this is, and if aging and HIV-infection have a synergistic effect on immune dysregulation.

During aging the immune system ages in a process called immune senescence. This process is characterized by a decrease in naïve T cell production and reduced T cell diversity resulting in a reduced ability to respond to infection [61, 62]. The decrease in generation of uneducated T cells from hematopoietic progenitors and the process of thymic involution during aging leads to a marked decline in naïve T cell production [63]. Indeed, when individuals of varying ages were compared there was a 95% decrease in thymic output from age 25 to age 60 [62]. For example, post radiation therapy there was a significant inverse correlation between age and sufficient renewal of CD4 T cell memory

subset, indicating reconstitution of a diverse memory subset required a diverse naïve T cell repertoire which was diminished or absent in older individuals [64]. By the age of 70 in otherwise healthy individuals, there is a significant skewing of the T cell population towards the memory phenotype (CD45RO-expressing CD4 T cells) and away from the naïve phenotype (CD45RA-expressing CD4 T cells), an increase in homeostatic proliferation of both naïve and memory CD4 T cells and an estimated loss of 99% of naïve T cell receptor diversity [62]. Some groups have found that instead of a slow decline, T cell receptor diversity appears stable until age 65-70, after which there is a significant drop in diversity [65]. This sudden decrease can be attributed to absent thymic activity in combination with loss of T cell homeostatic proliferative function, which plays quite a large role in maintaining the T cell population. Age-associated thymic involution leads to a decrease in thymic output and an increased dependence on peripheral T cell proliferation to maintain T cell homeostasis [66, 67].

HIV+ individuals, even during treatment, go through an ‘accelerated immune senescence’ which mirrors the immune senescence seen in the elderly [68]. HIV+ individuals are also known to present age-associated, non-AIDS-defining comorbidities more frequently or at younger ages than HIV- individuals. These comorbidities include, but are not limited to, osteoporosis, atherosclerosis, neurocognitive decline and cancer [69, 70]. Chronic inflammation induced in aging and HIV infection likely drive the morbidities and comorbidities observed in these populations, respectively [71, 72]. Also, the elderly population and the HIV+ population share the trait of poor immune response to vaccinations and infections [56, 58, 73, 74]. The CDC recommends an influenza vaccine for the elderly that has quadrupled the concentration of antigen per strain as the

standard vaccine. This same high-dose influenza vaccine has been also found to generate significantly higher antibody titers than the standard dose vaccine in the HIV+ population (88-90% on stable ART)[75].

MDSC have been found to be elevated separately in aging and HIV infection. Suppression of proliferative T cell responses by MDSC could be a major cause of impaired T cell homeostasis resulting in immune dysregulation in those who are both chronically infected and aging. We sought to address the role MDSC play in the cellular dysfunction associated with chronic retroviral infection in a virally-suppressed, aging host.

2.1 gMDSC frequency is elevated in older HIV+ men on antiretroviral therapy

HIV- (n=58) and HIV+ (n=57) individuals enrolled in our study (Table 1). The gender of our enrollment was skewed because while enrollment or recruiting was not restricted based on gender, we were able to obtain specimens from 40% male HIV- and 88% male HIV+ individuals. Data was not collected from nine specimens due to technical issues or specimen insufficiency. HIV+ individuals were median 51 years old (range 29-73) compared to the median age of 65 years old for HIV- individuals (range 30-92). HIV+ individuals were infected with HIV a median 14 years (range 6-31) with median CD4 counts of 559 (112-1388). Freshly isolated PBMC were stained for MDSC frequency and gMDSC were defined as CD11b+, CD14-, CD15+, CD33+, HLA-DR-, whereas mMDSC were defined as CD11b+, CD14-, CD15-, CD33+, HLA-DR-. Arginase-1 was stained intracellularly (Figure 2).

As we observed an elevation in MDSC frequency in women vs. men and at each age decade we restricted our analyses to HIV+ and HIV- men (Figure 3a-c). This was done to encompass the majority of the HIV+ donors.

MDSC frequency was significantly elevated in older (>50 years old) HIV+ vs. HIV- men. While MDSC elevation was observable at each age decade in HIV+ men, significance was only achieved for elevation of MDSC frequency in HIV+ individuals 60+ years of age (Figure 4a-b). Median gMDSC frequency was elevated in men with CD4 counts <350 cells/ml (Figure 4c).

	HIV-	HIV+
N=	58	57
% male	40%	88%
median (range)		
Age	65 (30-92)	51 (29-73)
Years HIV infected	N/A	14 (6-31)
CD4	N/A	559 (112-1388)

Table 1. Population demographics

PBMC were obtained from a total of 115 HIV- or virally suppressed HIV+ individuals of varying ages. HIV+ individuals were infected with HIV for at least 5 years (median 14 years) and virally suppressed for at least 1 year.

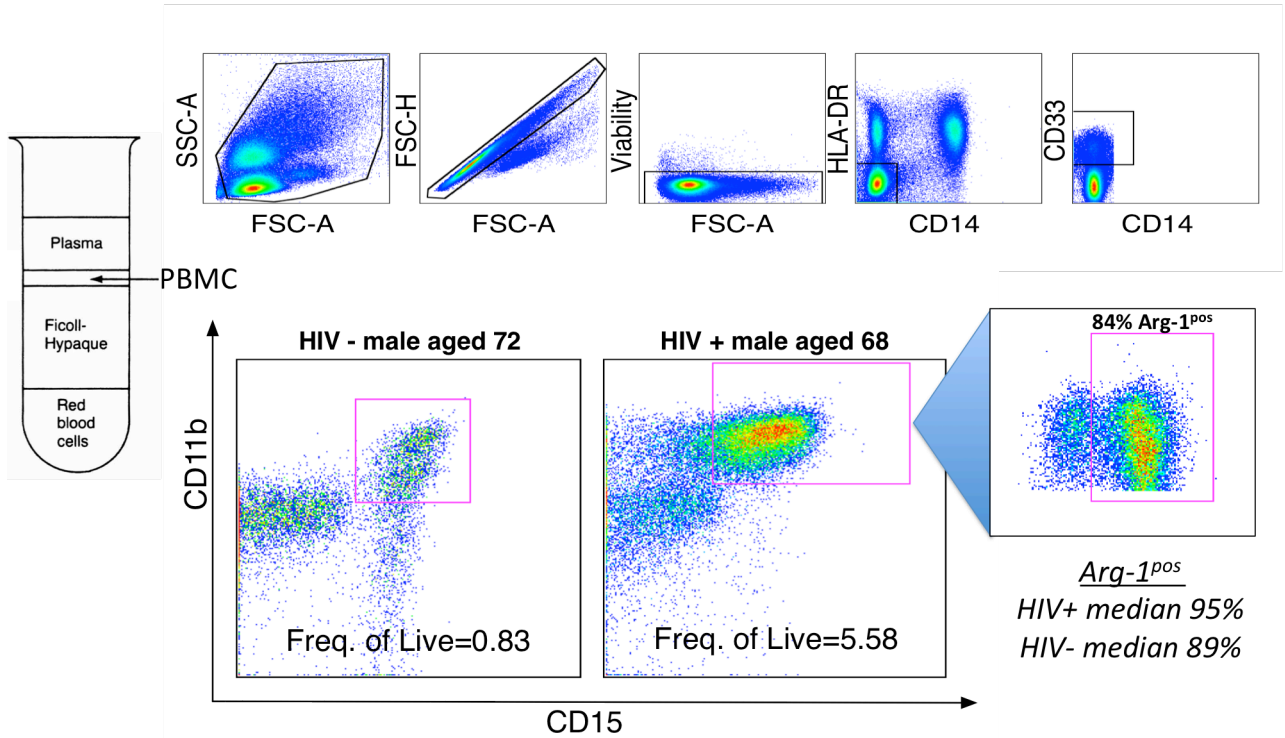


Figure 2. MDSC gating strategy and representative plots

Human gMDSC (granulocytic myeloid-derived suppressor cells) were defined as HLA-DR^{neg}, CD14^{neg}, CD33^{pos}, CD11b^{pos}, and CD15^{pos} while human mMDSC (monocytic myeloid-derived suppressor cells) were defined as HLA-DR^{neg}, CD14^{pos}, CD33^{pos}, CD11b^{pos}, and CD15^{neg}. Arginase-1 levels were measured by ICS.

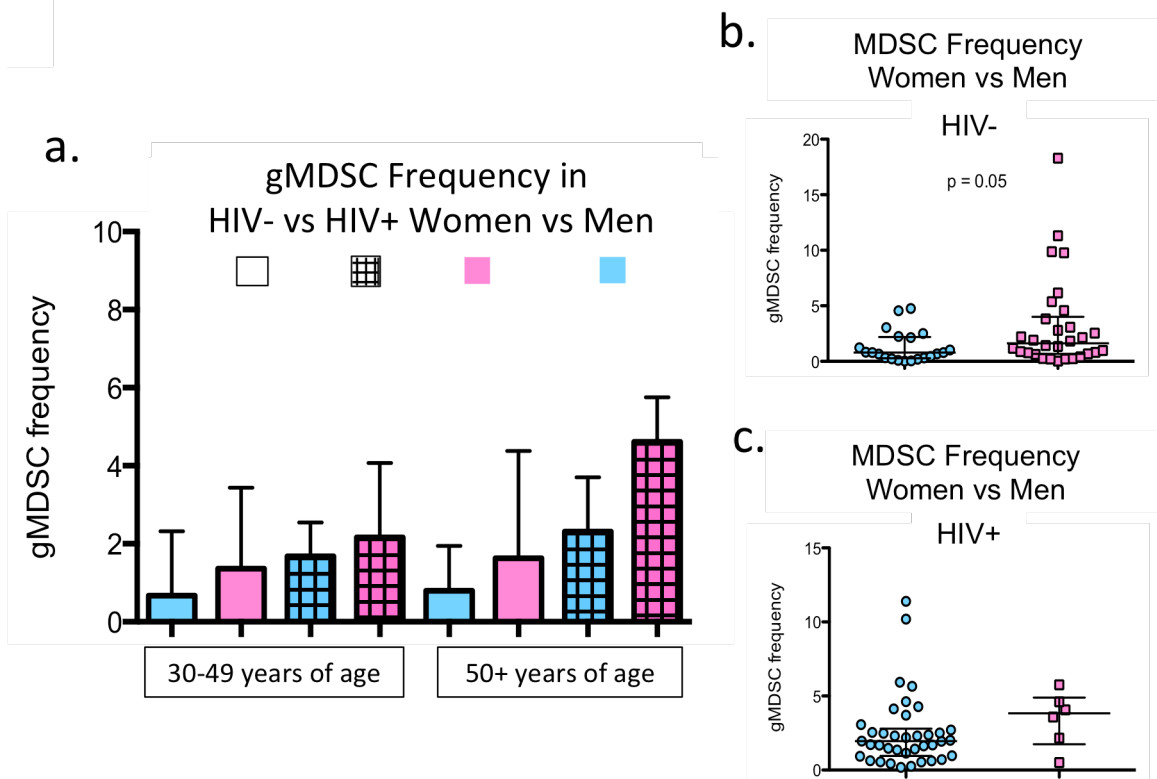


Figure 3. Women have higher MDSC frequencies than men

The gMDSC frequency of HIV- and HIV+ women vs. men was observably, but not significantly, different at each age decade group (A) and comparisons between men and women in total HIV- and HIV+ individuals (B-C) show a trend towards elevated gMDSC frequency in HIV- women vs. men. Median gMDSC were compared by Mann-Whitney U test.

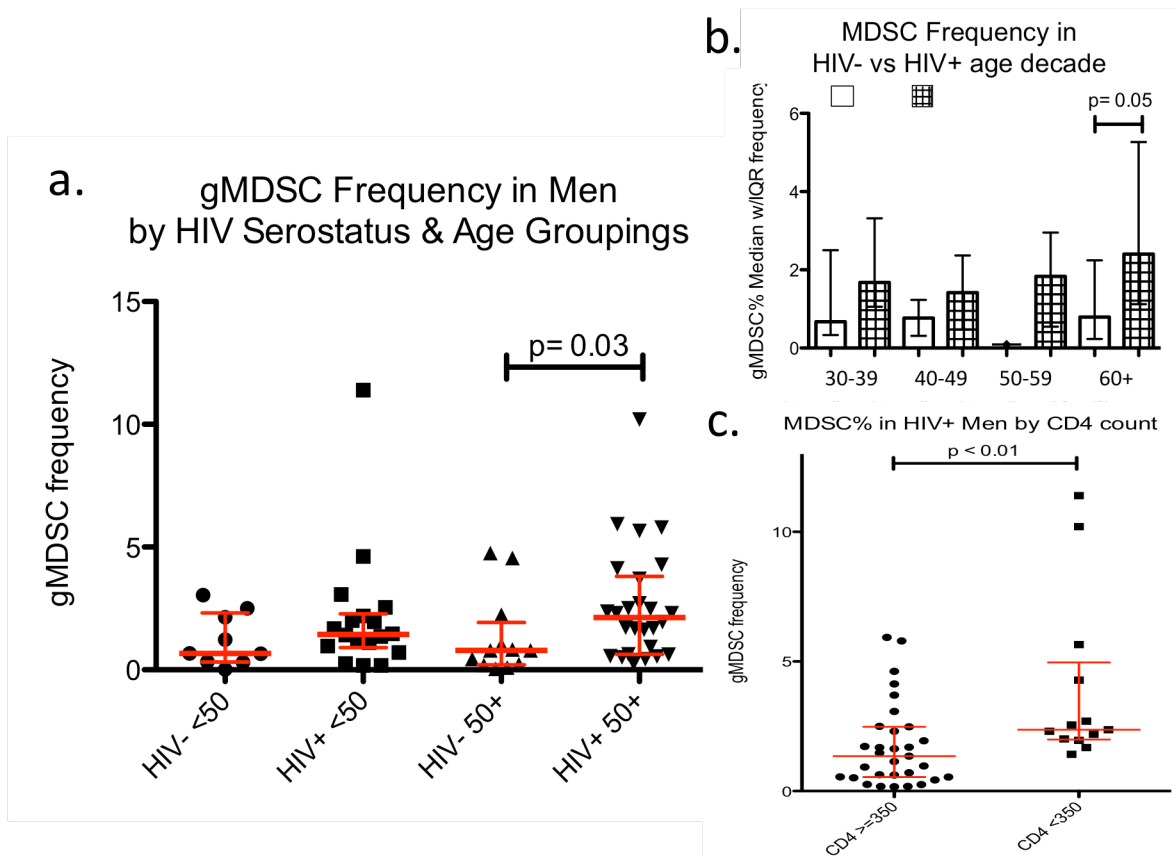


Figure 4. MDSC frequency is elevated in older HIV+ vs. HIV- men

Median gMDSC frequency of HIV- and HIV+ men under or over the age of 50 (A), by age decade (B), and by CD4 count \leq or ≥ 350 cells/ml (C), were compared by Mann-Whitney U test.

2.2 gMDSC suppress HIV Gag-specific responses

As granulocytes are thought to have short half-lives and do not survive cryopreservation, all work was done immediately post-blood draw. In our experimental model we determined via time course that gMDSC were 92% viable 24 hours post-culture (approximately 28-36 hours post-blood draw) and 49% viable 48 hours post-culture (approximately 52-60 hours post-blood draw) and concluded survival was sufficient to exert suppressive effects in a five-day culture. MDSC suppression was assessed by depleting these cells from total PBMC using anti-CD15 magnetic beads followed by stimulation of the total vs. MDSC-depleted PBMC with HIV Gag, CMV pp65 peptide pools or anti-CD3/CD28 beads (Figure 5a). When measured in this way the amount of MDSC suppression was quite variable. We observed significantly higher Gag-specific T cell proliferation when MDSC were depleted from PBMC; however, the magnitude of the Gag peptide response and degree of suppression varied from individual to individual (Figure 5b). We observed no significant suppression by MDSC of CMV-specific or polyclonal T cell proliferative responses (Figure 5c-d).

2.3 gMDSC require contact or proximity to exert suppressive effects

Transwells® were utilized to separate MDSC from directly contacting PBMC in five independent experiments in five individuals. MDSC suppression was observed in four experiments. MDSC effects were abrogated by transwell® insert between stimulated MDSC-depleted PBMC and MDSC (Figure 6a). This suggested either contact dependence or close proximity dependence, so we investigated mechanisms that require

either contact or proximity. Arginase-1, present in the majority of gMDSC observed (median 89% and 95% for HIV- and HIV+ individuals, respectively), is one of the main contributors to gMDSC-mediated suppression (discussed in Chapter 1.2), and may require close proximity in order to deplete arginine in the microenvironment. However, adding 10x physiologic levels of arginine to the culture (arginine-rescue) did not abrogate MDSC-mediated T cell suppressive effects in two independent experiments (Figure 6b-c). We then targeted ROS, another well-characterized mechanism by which gMDSC have been found to suppress T cells. Experiments testing inhibition of both ROS and arginase-1 were inconclusive as they were performed on HIV Gag peptide pool or CMV pool stimulated PBMC in a participant who did not have measurable peptide responses to either stimulus (data not shown).

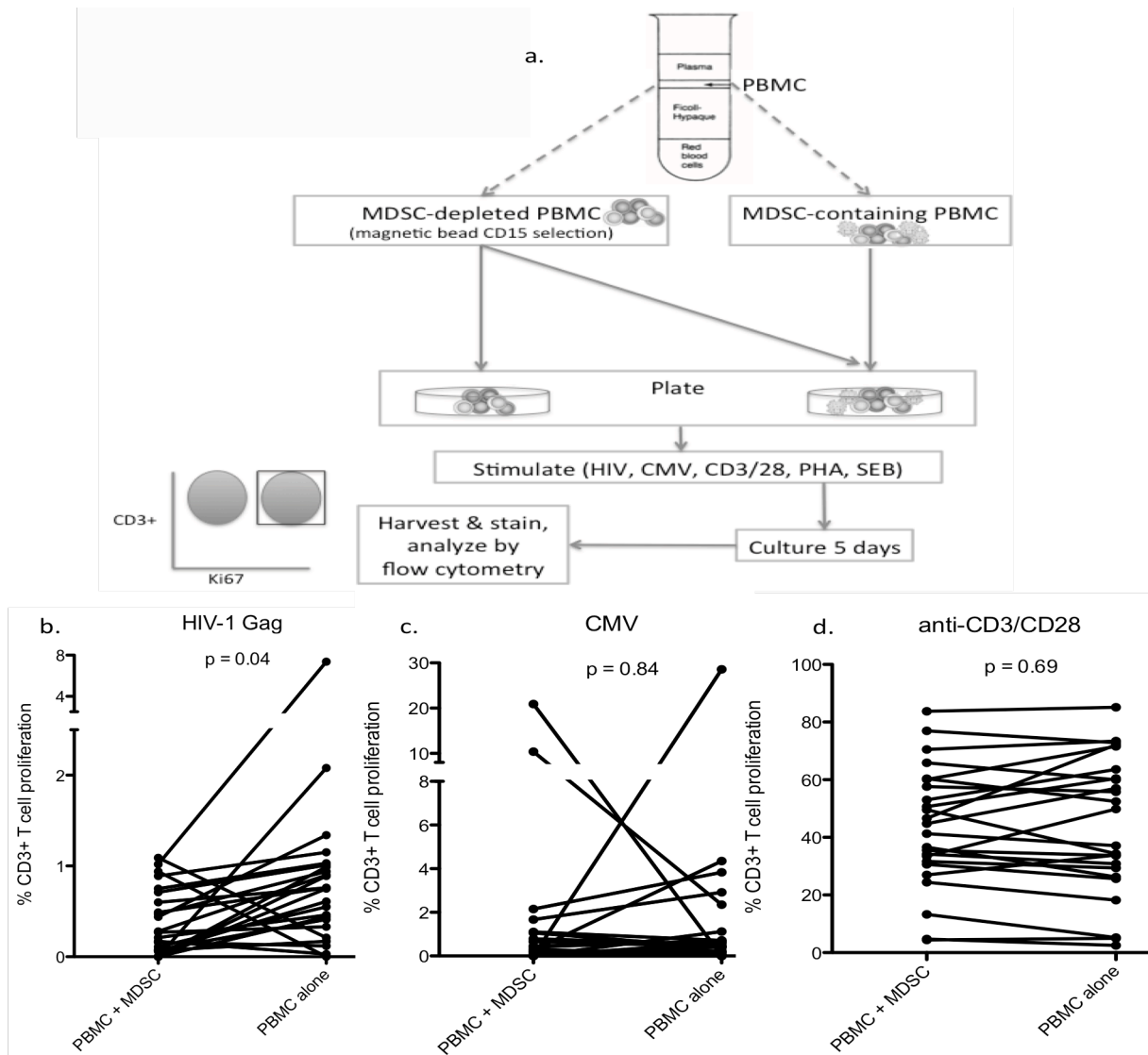


Figure 5. MDSC suppress HIV Gag, but not CMV or polyclonal, stimulated T cell proliferation

CD15+ MDSC were depleted via magnetic bead separation from PBMC (A). CD15-depleted PBMC (PBMC alone) or un-depleted PBMC (PBMC+MDSC) were stimulated with either 2ug/ml HIV Gag peptide pool (B), 2ug/ml CMV pp65 peptide pool (C), 10ul/ml Dynabeads CD3/28 (D) then cultured at 37°C, 5% CO₂, for five days. T cell proliferation was measured by ICS for Ki67 and CD3. Proliferation levels in PBMC+MDSC vs. PBMC alone were compared by Wilcoxon signed rank test.

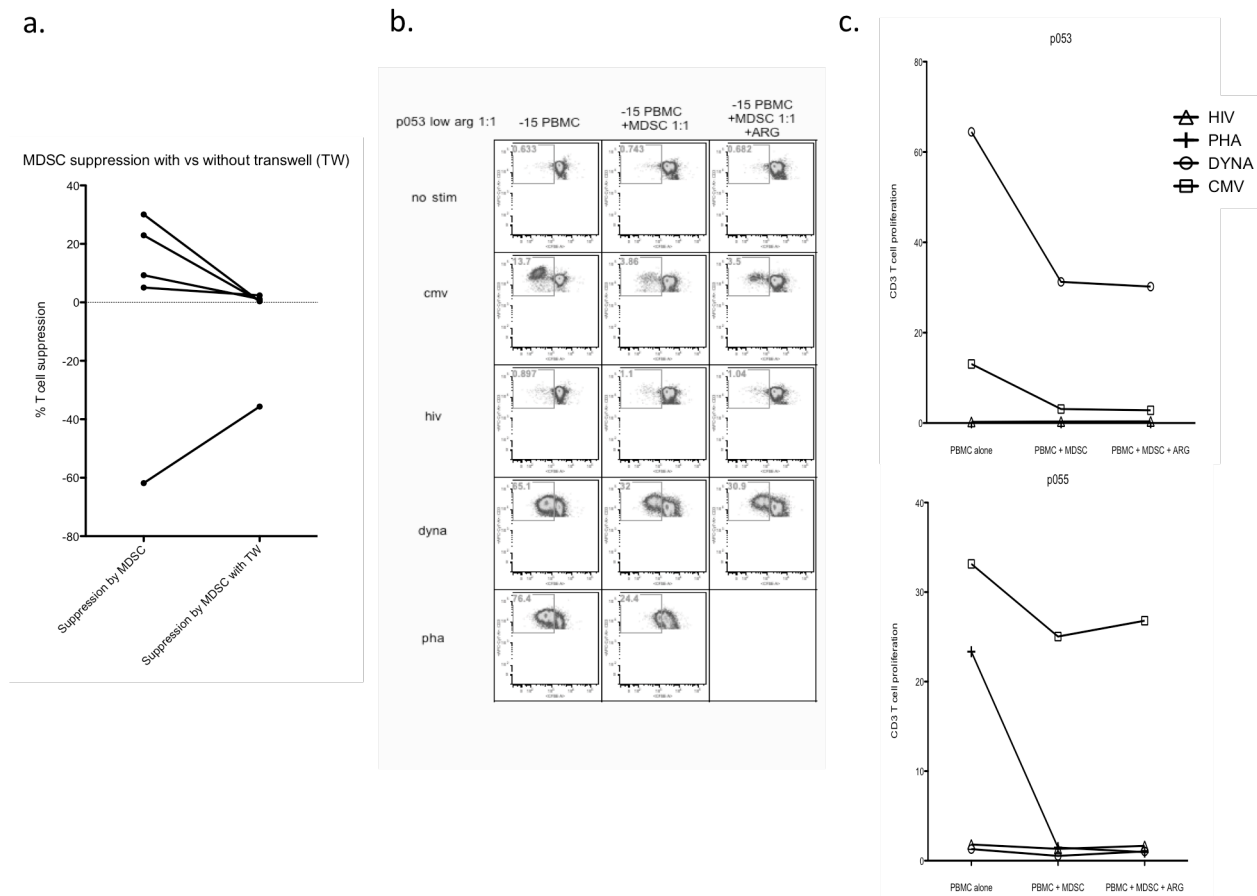


Figure 6. Transwell® abrogates MDSC suppressive function while arginine rescue has no effect

CD15+ MDSC were separated from total PBMC using CD15 magnetic bead isolation. CD15+ MDSC fraction was added back to the CD15- PBMC either in the same well or in the same well separated by a Transwell® both at a 1:1 PBMC:MDSC ratio and stimulated with 10ul/ml Dynabeads CD3/28 (A). Arginine rescue experiments were performed in 1.15mM L-arginine monohydrochloride and stimulated with 2ug/ml pooled HIV Gag 15mer overlapping peptides, 2ug/ml CMV pp65 peptide pool, 10ul/ml Dynabeads CD3/28, 0.4ug/ml Staphylococcal enterotoxin B or 2ug/ml PHA (B-C). Experiments were cultured at 37°C, 5% CO₂ for five days in custom arginine-low media.

2.4 Inflammatory cytokines correlate with gMDSC levels

Plasma was tested by multiplex ELISA for GM-CSF, M-CSF, G-CSF, SCF, FLT3-L, CD14, IFN γ , IL-1 β , IL-6, IL-10, TNF α , VEGF and CRP. We observed weak trends towards correlations between total MDSC frequency and VEGF, IL-6, IL-1 β , FLT-3L and CRP (Figure 7). Thinking that there may be additive effects on the MDSC population by the total cytokine milieu we were missing by looking at each factor individually, we ranked levels of factors known to expand (IL-6, VEGF, IL-1 β , IL-10, FLT3-L, SCF, G-CSF, GM-CSF) or activate (IFN γ , IL-1 β , IL-10, VEGF, IL-6, G-CSF) the MDSC population. When we ranked and tallied expanders and activators we found that expanding, but not activating, cytokines correlated with total MDSC frequency (Spearman $r=0.53$, $p<0.0001$) driven more by the granulocytic (Spearman $r=0.53$, $p<0.0001$) than monocytic (Spearman $r=0.25$, $p=0.08$) subset. Using this same ranking system we examined suppressive ability of gMDSC correlated to activating cytokines and observed suppression of either CD3/28 or Gag peptide stimulus did not correlate with the activating cytokines (data not shown).

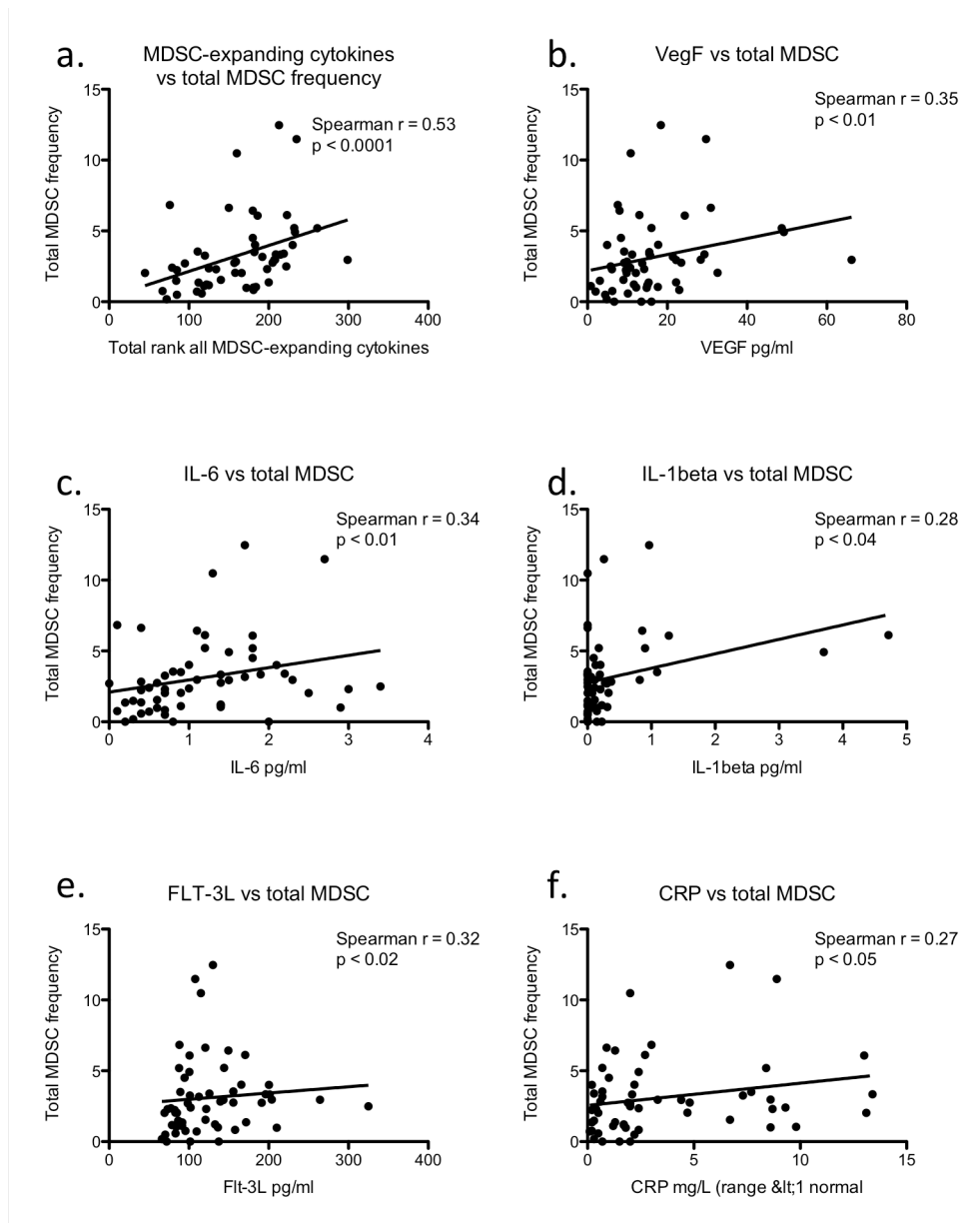


Figure 7. MDSC levels correlate with MDSC-expanding cytokines

Plasma was batch tested as per kit instructions using R&D systems 6-plex for GM-CSF, M-CSF, G-CSF, SCF, Flt-3 L, and CD14, 6-plex for IFN γ , IL-1 β , IL-6, IL-10, TNF α and VEGF and 1-plex for CRP. Cytokines known to expand or activate MDSC subsets were correlated with MDSC frequency or suppression, respectively. Ranked levels of factors known to expand (IL-6, VEGF, IL-1 β , IL-10, FLT3-L, SCF, G-CSF, GM-CSF) or activate (IFN γ , IL-1 β , IL-10, VEGF, IL-6, G-CSF) the MDSC population were compared to MDSC frequency (A) and suppression (data not shown). Individual correlations were found between MDSC frequency and VEGF, IL-6, IL-1beta, FLT-3L and CRP by Spearman's rank correlation coefficient.

2.5 Discussion

We observed a significant increase in gMDSC, not mMDSC, frequency in our HIV+ vs. HIV- individuals. For our study we chose to enroll individuals on successful suppressive therapy since these individuals comprise the majority of the HIV+ aging population. The population selected for study may be driving the MDSC subset elevation observed. Although our enrollees' were older (average age of 50), their general health was similar to the two studies reporting increases in gMDSC frequency as they had relatively high CD4 counts (median >500, range 112-1053) and were in good health. We only assessed four individuals with CD4 counts below 200 and cannot adequately compare the mMDSC frequency of this group to those with higher CD4s; however, it is interesting to note that the one individual with the lowest CD4 count (112 CD4/ul) also had the highest mMDSC frequency (5.65%).

We observed elevations in frequency of MDSC in older HIV+ vs. HIV- men driven by the granulocytic subset. MDSC frequency has been found to be elevated in aging mice [76] and humans [49]. Elevated MDSC have been found in HIV+ individuals that decrease post-HAART therapy. Granulocytic MDSC were more frequent in HIV+ populations with better health measured by higher CD4 counts and lower clinical stage of infection. All the HIV+ individuals were on suppressive therapy and had relatively high median CD4 counts, so it is not surprising that there were observable, but not significant, elevations between the younger (30-49 years old) HIV+ vs. HIV- men. In the older HIV+ vs. HIV- men where we observed a significant difference, we hypothesize that both aging and HIV infection contribute to the cumulative exposure of inflammatory cytokines driving MDSC expansion and activation.

Cytokine data suggests a role for IL-6, VEGF, IL-1 β , FLT3-L individually, but more important may be the aggregation of low levels of many of the MDSC-expanding inflammatory cytokines. Initial work elucidating the importance of individual cytokines has been performed primarily in mouse tumor models. In these models it is clear that these cytokines are tumor-derived and cause downstream activation of STAT3, the well-described MDSC master transcription factor (reviewed in [1]). In humans, MDSC have been found to have increased STAT3 phosphorylation correlating with arginase-1 levels and suppressive activity [77]. Interestingly, we did not observe correlations between suppressive ability and known MDSC activators, individually or together. Known expanders and activators of MDSC we did not assay for directly are TLR ligands. TLR ligands signal through NF- κ B to promote MDSC activation and mobilization from the bone marrow. MDSC induction is thought to be MyD88-dependent (reviewed in [1]). As MyD88 is important for sensing of HIV through TLR 7, 8 and 9 (reviewed in [78]) and sensing the products of microbial translocation through TLR 2, 5, 6 and 9 [79, 80] there may be a role for either low-level viral replication or the products of microbial translocation signaling through TLRs in activation of MDSC. Although the individuals we enrolled were all virally suppressed, they each likely had different basal low levels of replication and microbial translocation driving the MDSC activation status.

Experimentation with MDSC to determine a mechanism of suppression in our human subjects was difficult for a few reasons. MDSC yield depended on the frequency in each individual, PBMC responses to each stimulus was variable and MDSC frequency and function was variable subject to subject. We did not observe consistent suppression post polyclonal stimulation of T cells, and while we observed significant suppression of

HIV Gag peptide responses, very few individuals responded to this peptide pool with over 1% proliferation. The low yield of MDSC and extreme experimental variability made it very difficult to examine the role of inhibitors of known mechanisms of suppression.

The person-to-person variability we observed could have occurred for any number of reasons as there are known exposures that drive activation and expansion of MDSC that we did not, or could not, account for in a human model. Alcohol use and abuse, obesity and smoking are common in the United States (7% alcohol use disorder, 30% obese, 16.8% smoking) and evidence suggests these exposures drive expansion of the MDSC subset. In obese individuals higher circulating levels of estrogen and the inflammatory cytokines $\text{TNF}\alpha$, IL-6, IL-1 β and IL-12 have been observed and, indeed, there was marked accumulation of MDSC in a mouse obesity model (reviewed in [81]). Chronic alcohol use in a mouse model has been found to expand a population of MDSC that suppress CD8 T cells [82]. Carcinogenic smoke exposure in a mouse model induced a population of MDSC-like cells that predated tumor development, and post-tumor these cells acquired potent suppressive function characteristic of true MDSC [83]. Lastly, it has been shown in a mouse model that activation of the cannabinoid receptor can expand and activate MDSC [84].

HIV+ individuals are much more likely to smoke (as many as 50-70% reviewed in [85]) and have alcohol use disorders (29-60% reviewed in [86]) than the general population and are approaching overweight/obesity rates similar to the general population (46% overweight, 17% obese in [87]), and some may have been prescribed or use marijuana recreationally. Therefore, variations in these exposures may have driven the

wide range of MDSC frequency and function observed. We did not include survey data on weight at blood draw or the exposure to alcohol, cigarette smoke or marijuana. Had data been collected for these exposures, including the variables of age, age at HIV acquisition, length of HIV infection prior to viral suppression, duration of viral suppression and history of cART regimen in our subjects, the extreme variability in the potential combination of exposures would have likely precluded any conclusive analyses.

In summary, this work focused on characterizing MDSC in HIV+ individuals on cART at varying ages. We examined MDSC frequency and functionality in over 100 individuals and found elevation of MDSC in older HIV+ vs. HIV- individuals. These MDSC suppressed HIV-specific T cell responses and correlated with inflammatory cytokines implicated in MDSC accumulation. We did not identify a putative mechanism of MDSC-mediated T cell suppression but preliminary experimental data suggests contact dependence independent of arginase-1 and nitric oxide. Further work examining both the mechanism of MDSC-mediated suppression and therapies to address elevated inflammation in the aging HIV+ population are warranted.

Chapter 3: Kinetics of myeloid derived suppressor cell frequency and function during SIV infection, combination antiretroviral therapy and treatment interruption

3.0 Introduction

Myeloid-derived suppressor cells are a heterogeneous group of immunosuppressive cells of myeloid origin. Myeloid-derived suppressor cells were originally described, and have canonically been characterized, in mouse tumor models and cancer patients where they inhibit anti-tumor responses and correlate with poor clinical outcomes. When MDSC are ablated, either natural immunity or chemotherapeutic agents have been found to be more efficacious. Myeloid-derived suppressor cells inhibit T cell responses to a myriad of stimuli in a myriad of ways (reviewed in [2]).

During pathogenic retroviral infections including HIV and SIV, cellular and humoral immune responses are insufficient to clear acute infection, leading to disease progression for most individuals. In these individuals, despite initial effective cellular responses critical for viral control, T cells lose functional capacity leading to disease progression [43]. A small subset of individuals called HIV controllers maintain T cell polyfunctionality and proliferative ability, retaining the ability to control viral replication and disease progression in the absence of antiretroviral therapy. Of T cell functions, loss of proliferative ability in response to HIV-stimulation is the strongest independent predictor of progression vs. control [44]. Systemic inflammation is a hallmark of chronic pathogenic retroviral infections and contributes greatly to the immune dysfunction observed. In retroviral infection chronic systemic inflammation is induced via viral replication and microbial translocation and is dampened but persists during virologic

suppression [45, 46]. Indeed, immune activation correlates stronger with poor prognosis than viral load or co-receptor use alone [47].

The causes of T cell dysfunction in progressive infection and the link between cellular dysfunction and immune-activation dependent disease outcomes are not yet completely understood. Inflammation during acute infection serves to drive and tune the innate and adaptive immune responses but persists as these responses are insufficient to resolve viral replication. Additionally, microbial translocation due to loss of gut barrier integrity continues to drive inflammation even in the absence of viral replication. We suspect MDSC are expanded and activated due to inflammation resulting from viral replication and microbial translocation and that, subsequently, these MDSC contribute to immune exhaustion by suppressing the proliferative capacity of virus-specific T cells.

Previous studies showed increased frequencies of gMDSC and mMDSC in HIV+ vs. HIV- individuals that correlated with high viral loads, low CD4 counts, increasing T cell activation and advanced disease stage [35-37]. In SIV infection, studies have shown a CD8-T cell suppressive mMDSC-like population of monocytes in a pigtailed macaque (*Macaca nemestrina*) SIV infection model that decrease in frequency during cART treatment [41]. MDSC have been studied in the context of prophylactic SIV vaccine and were significantly elevated in the vaccination but not in the control group, which displayed better virologic control and no less protection from infection compared to the vaccinated group. This suggests MDSC were in fact elicited by in the vaccine, hampering immune control of SIV. These MDSC suppressed CD8 proliferative responses to SIV in a dose-dependent manner and correlated with higher set-point viral load.

As these studies were either cross-sectional or had a limited sampling timeline, the pervasiveness, activity and clinical consequences of MDSC over the course of infection are unknown. In addition, it is not clear if elevations in MDSC frequency predate the acquisition of virus. Also uncertain is the impact of cART treatment interruption on MDSC populations. We followed seven animals over the course of SIV infection, treatment with cART and cART interruption to examine the kinetics of MDSC frequency, their function in chronic retroviral infections and their relationship to T cell activation and inflammatory cytokine responses. Here we show gMDSC are elevated and suppressive in acute and cART-treated chronic retroviral infection. At cART-interruption we show a marked increase in gMDSC that correlates significantly with a secondary and enhanced inflammatory cytokine elevation.

3.1 MDSC frequency is elevated at all stages of SIV infection

MDSC frequency was determined in two populations of rhesus macaques: a pilot study of chronically SIV infected animals at 12 weeks post-infection and a longitudinal study of uninfected animals that was followed over the course of SIV infection (Figure 8a). During the pilot study a flow cytometry panel was optimized to identify MDSC of granulocytic (gMDSC) or monocytic (mMDSC) origin in the Rhesus macaque model. MDSC were defined as singlet cells that were CD3⁻, CD11b⁺, HLA-DR⁻, and for gMDSC, CD66⁺, SSC^{mid-high} while for mMDSC, CD66⁻ and CD14⁺ (Figure 8b).

We observed elevated frequencies of MDSC ($p=0.03$) in five chronically-SIV infected animals at 12 weeks post-infection (Figure 9a). Total MDSC (Spearman $r=0.90$,

p=0.08) and gMDSC (Spearman $r=1.00$, $p=0.02$) frequencies correlated with viral load set-point (Figure 9a-b).

We next embarked on a longitudinal study where we observed low MDSC frequency (median 0.18%) at pre-SIV time-points in seven animals that increased slightly, yet significantly, during acute infection at two to three weeks post-SIV challenge (median gain of 0.51%; Figure 10a-c). Combination antiretroviral therapy was initiated six weeks post-infection and MDSC frequency remained elevated during cART with transient blips in A14047 and A14048 at weeks 14 and 36 (A14046) and 18 (A14047) (Figure 11). For clarity we included only summary data (Figure 10) when all animals had achieved viral suppression, and then individually graphed the viral load kinetics vs. MDSC frequency for each animal adjacent to the CD4 kinetics (Figure 11). The CD4 levels did not correlate with MDSC frequency (data not shown).

At 37 weeks (after 31 weeks on cART), drug therapy was withdrawn and MDSC were monitored to determine the effects of drug interruption on MDSC responses. Results in Figure 10a show MDSC increased dramatically (median gain of 6.8%) over the first 20 weeks post-cART interruption. Although the drastic increase in MDSC frequency after stopping cART was transient, MDSCs remained elevated at 30 weeks post-cART interruption when compared to pre-SIV infection levels. Animals A14044 and A14047 (Figure 10-11†) were euthanized due to AIDS-defining illnesses before study completion. Elevations in MDSC frequency were comprised primarily of the granulocytic subset of MDSC (gMDSC median 88% of total MDSC observed) (Figure 10b). Monocytic MDSC were infrequent in our study, only increasing significantly from baseline at 20 weeks

post-cART. This increase was much less (median gain of 0.26% from baseline) and also transient, returning to pre-SIV levels at week 68 (Figure 10c).

In order to show that increased frequencies of MDSC were not driven by changes in the frequencies of other cell subsets within the PBMC, we measured absolute numbers of MDSC. MDSC cells per ul blood, determined by Countbright™ Absolute Counting Beads, tightly correlated with total MDSC (Figure 12a) as well as gMDSC and mMDSC frequency (Figure 12b-c). MDSC cells per ul blood mirror the kinetics of MDSC frequency in SIV infection (Figure 12d vs. Figure 11a).

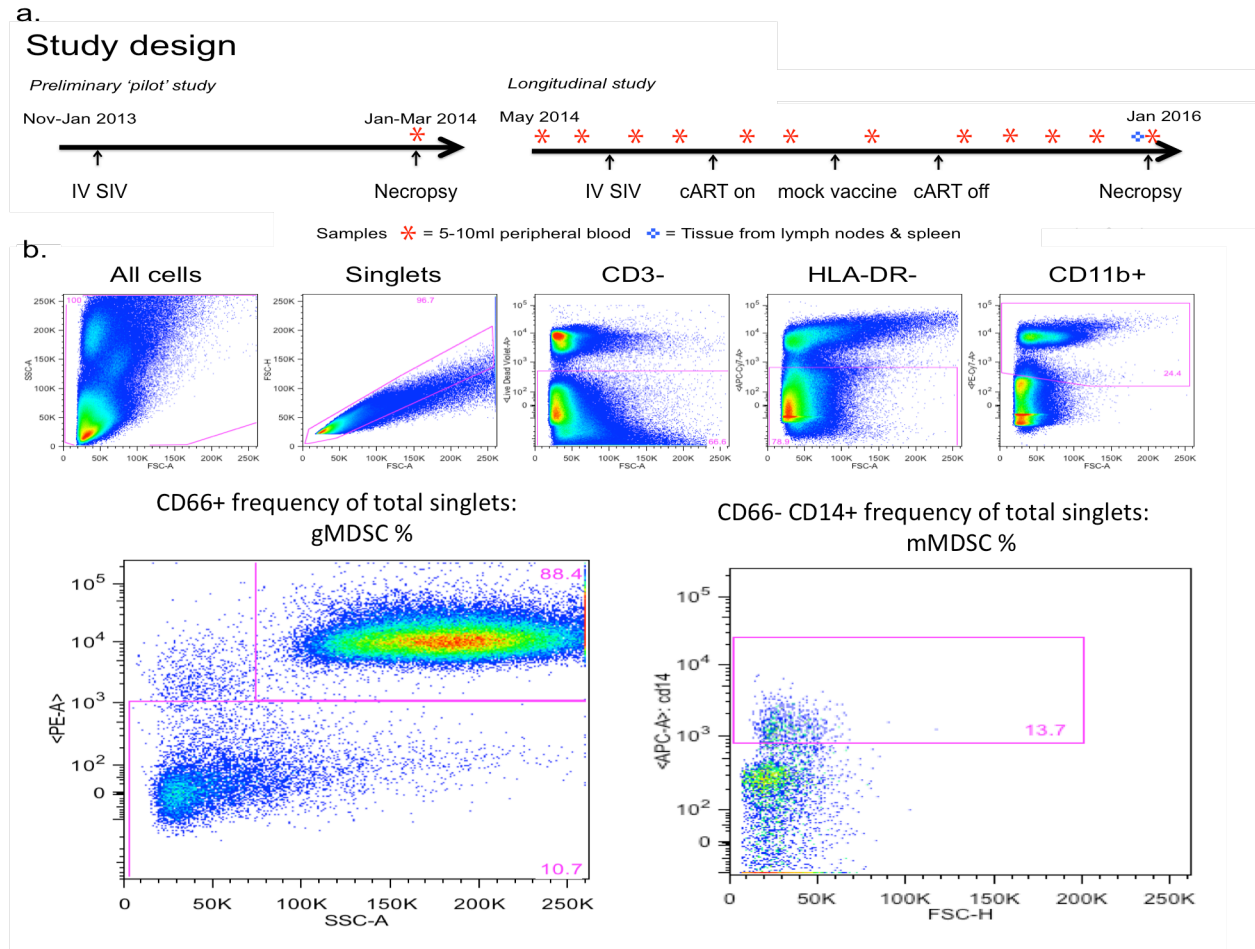


Figure 8. Study design and MDSC gating strategy

Rhesus macaque (*Macaca mulatta*) blood and tissue were obtained from the Washington National Primate Research Center (WaNPRC). Pilot study blood draws were obtained 12 weeks post-SIV infection with no combination antiretroviral therapy (cART). Longitudinal study animals were infected IV with SIV/DeltaB670 at week 0 and put on cART 6 weeks post-infection. From 18 weeks to 30 weeks post-infection the animals were mock vaccinated with empty plasmid vector +/- LT adjuvant. At 37 weeks post-infection all animals had achieved viral suppression and were taken off cART. The animals were then followed until week 80 or until AIDS-defining illness. Longitudinal study blood draws were obtained pre-SIV infection at weeks -4 and -3, and at weeks 2, 3, 10, 14, 18, 36, 37, 40, 46, 56, 68 post-infection and blood and tissue was obtained at necropsy (A). Rhesus macaque gMDSC were defined as HLA-DR^{neg}, CD14^{neg}, CD11b^{pos}, SSC^{mid/high} and CD66^{pos} while mMDSC were defined as HLA-DR^{neg}, CD14^{pos}, CD11b^{pos}, and CD66^{neg} (B).

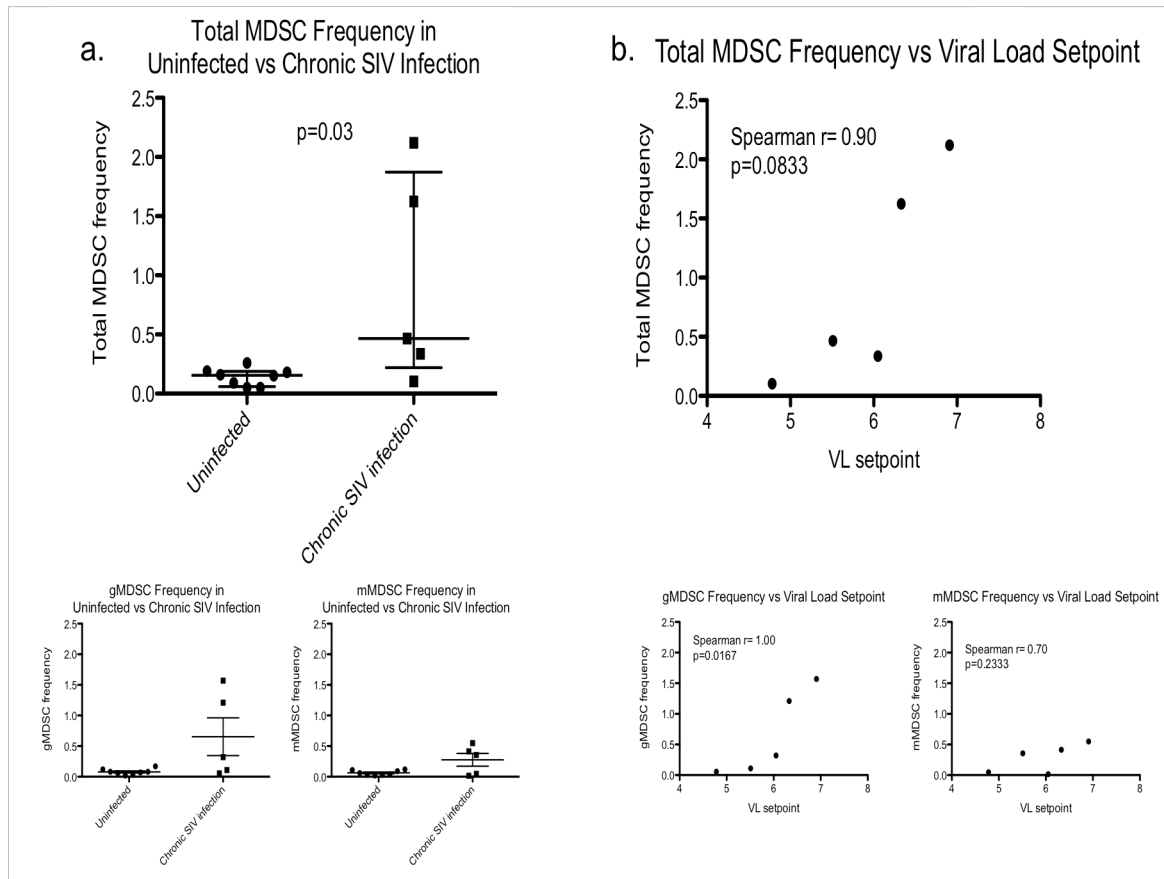


Figure 9. Myeloid-Derived Suppressor Cell Frequency in Chronic SIV infection: Pilot study

MDSC frequency was determined 12 weeks post-SIV infection in both gMDSC and mMDSC subsets in SIV chronically infected animals ($n=5$) (A) and correlated with set-point viral loads (B). Median MDSC frequencies were compared by Mann-Whitney U test and viral loads were correlated to MDSC frequencies by Spearman's rank correlation coefficient.

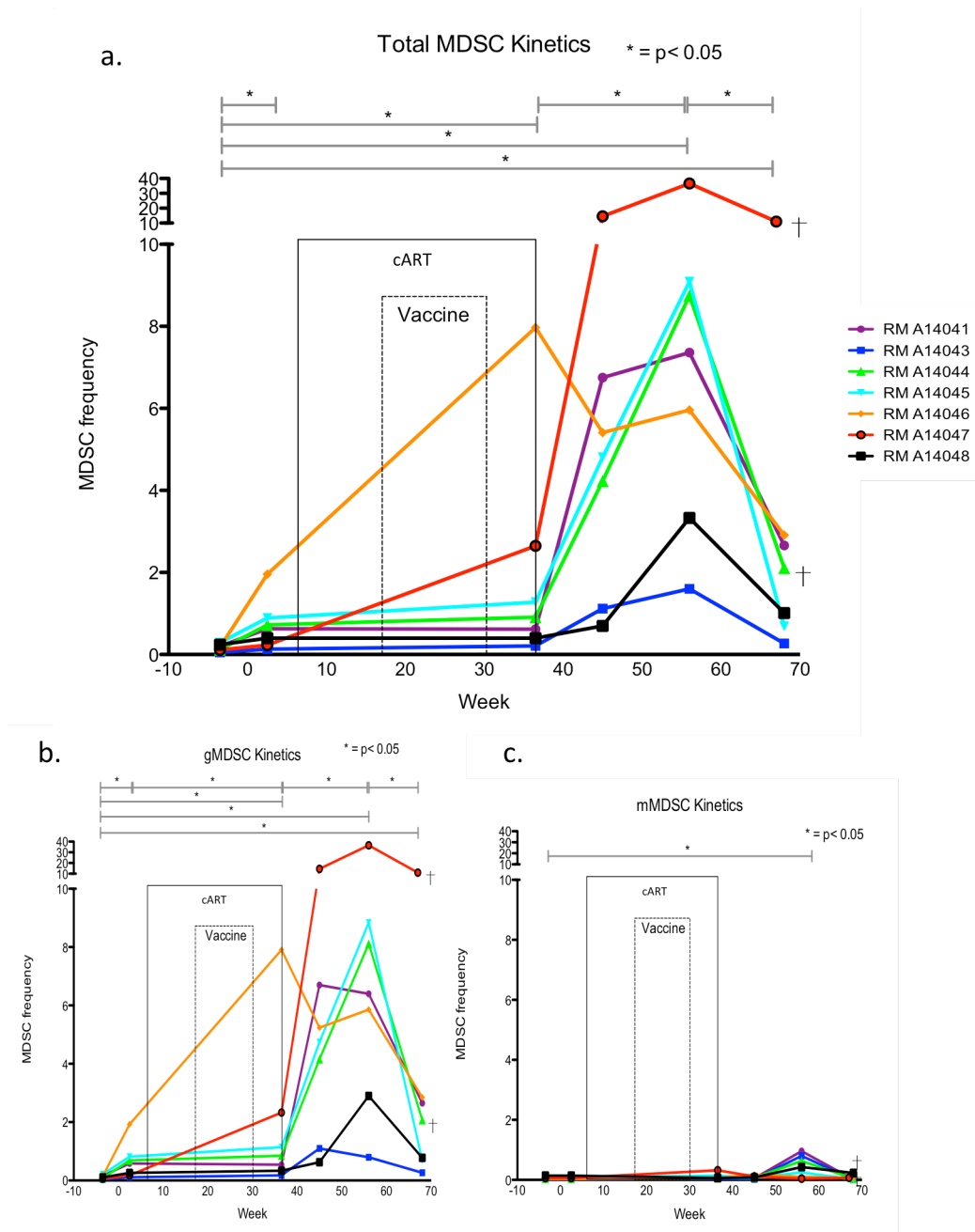


Figure 10. Myeloid-Derived Suppressor Cell Frequency in Chronic SIV infection: Longitudinal Study

Total MDSC frequency was measured in uninfected animals ($n=7$) then followed post-SIV challenge (week 0), during cART, and post-cART (A). Both the granulocytic (gMDSC) and monocytic (mMDSC) fraction of the total MDSC population were measured to determine their individual kinetics during infection (B-C). Animals A14044 and A14047 were euthanized due to AIDS-defining illnesses before study completion (†). For clarity summary data during cART includes only time-points where all animals were virally suppressed, as time to viral suppression on cART was variable. MDSC frequencies were compared by Wilcoxon signed-rank test.

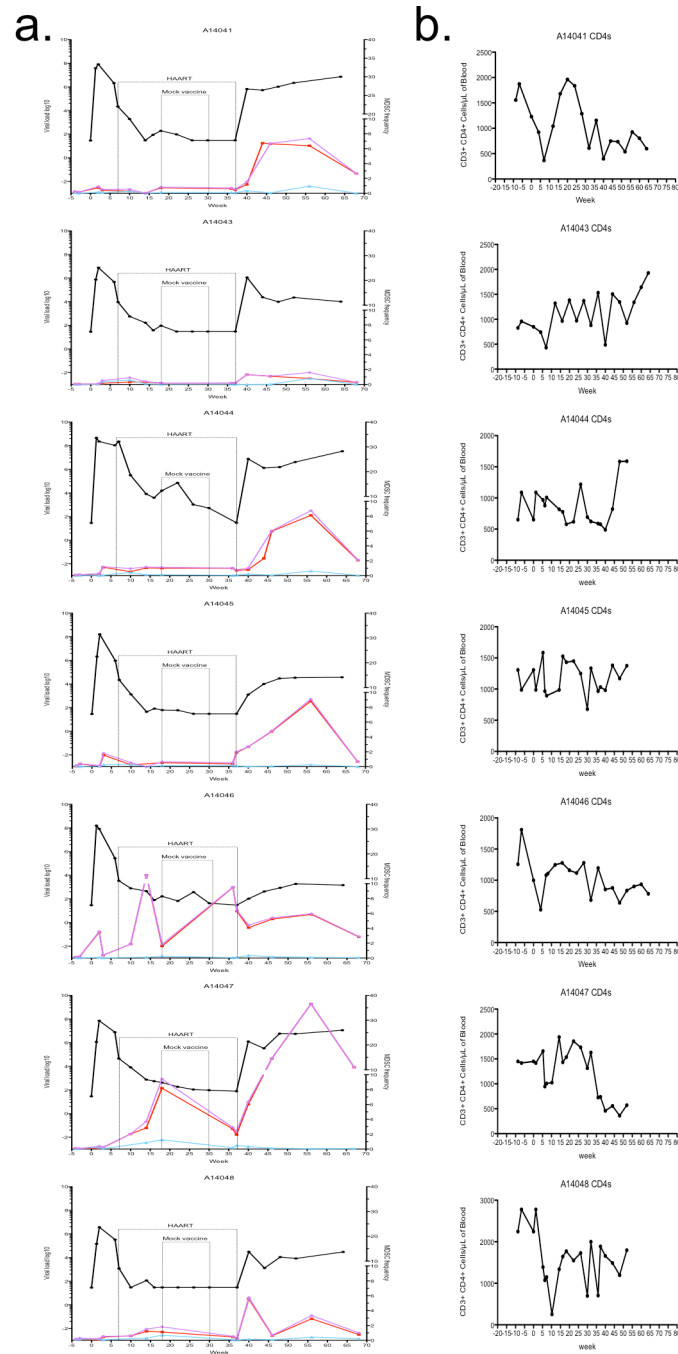


Figure 11. Individual Viral load, MDSC Frequency and CD4 Kinetics

Individual SIV viral load kinetics (in black) were charted with total MDSC frequency (purple), gMDSC frequency (red) and mMDSC frequency (blue) (A). CD4 count kinetics were plotted to the right of each MDSC graph (B).

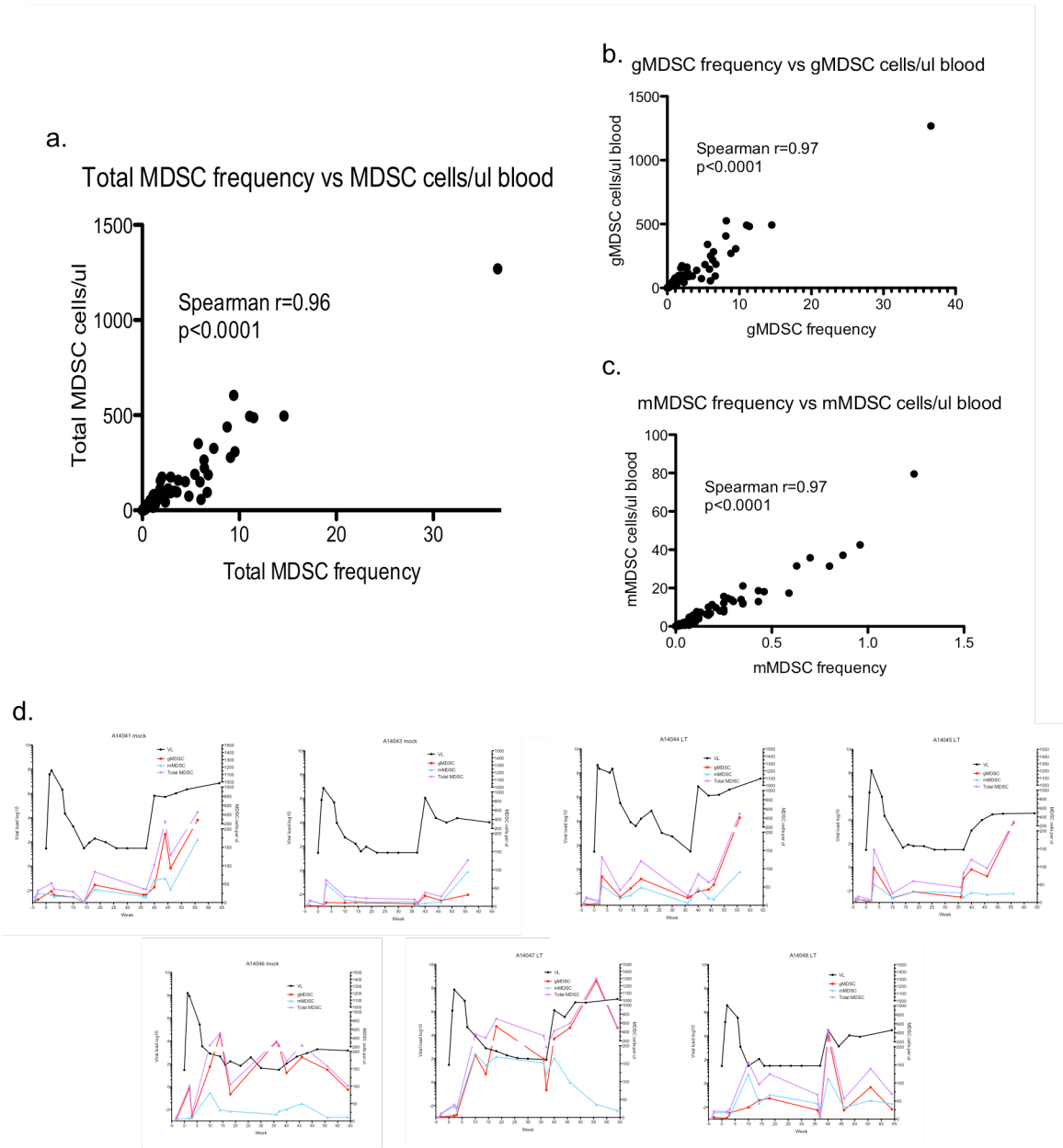


Figure 12. MDSC frequency of cells correlates tightly with cells/ul blood

Total MDSC cells per ul blood (A) as well as gMDSC (B) and mMDSC (C) correlate with MDSC frequency in singlet cells. MDSC cells/ul blood kinetics in SIV infection (D). MDSC cells per ul blood determined using CountBright™ Absolute Counting Beads in whole blood in combination with whole blood (CD45, CD66) and MDSC (CD3, CD11b, CD14, CD16, CD66, HLA-DR) staining panel. MDSC frequency was correlated with cells per ul blood by Spearman's rank correlation coefficient.

3.2 MDSC suppress SIV-specific and polyclonally stimulated T cell responses

To determine the effects of MDSC on T cell responses we cultured PBMC in the presence or absence of MDSC with SEB or SIV Gag peptide pools (Figure 13a). T cell proliferation, measured by Ki67, was suppressed in PBMC+MDSC wells compared to PBMC alone. We assayed the suppressive ability of MDSC for each animal three weeks pre-SIV infection, three weeks post-SIV infection, during cART (31 weeks after starting cART) and 19 weeks after stopping cART. We found significant suppression by MDSC of SEB-stimulated responses at all time-points (Figure 13c) and in the presence of SEB, both CD4 and CD8 cell subsets were suppressed (Figure 13d). SIV peptide responses were variable over the course of the study (Figure 13e), but at those time-points where a sufficient response ($>0.5\%$) was detected, we observed significant suppression of SIV-specific T cell responses by MDSC (Figure 13f). MDSC suppressive effects were dose dependent (Figure 13g).

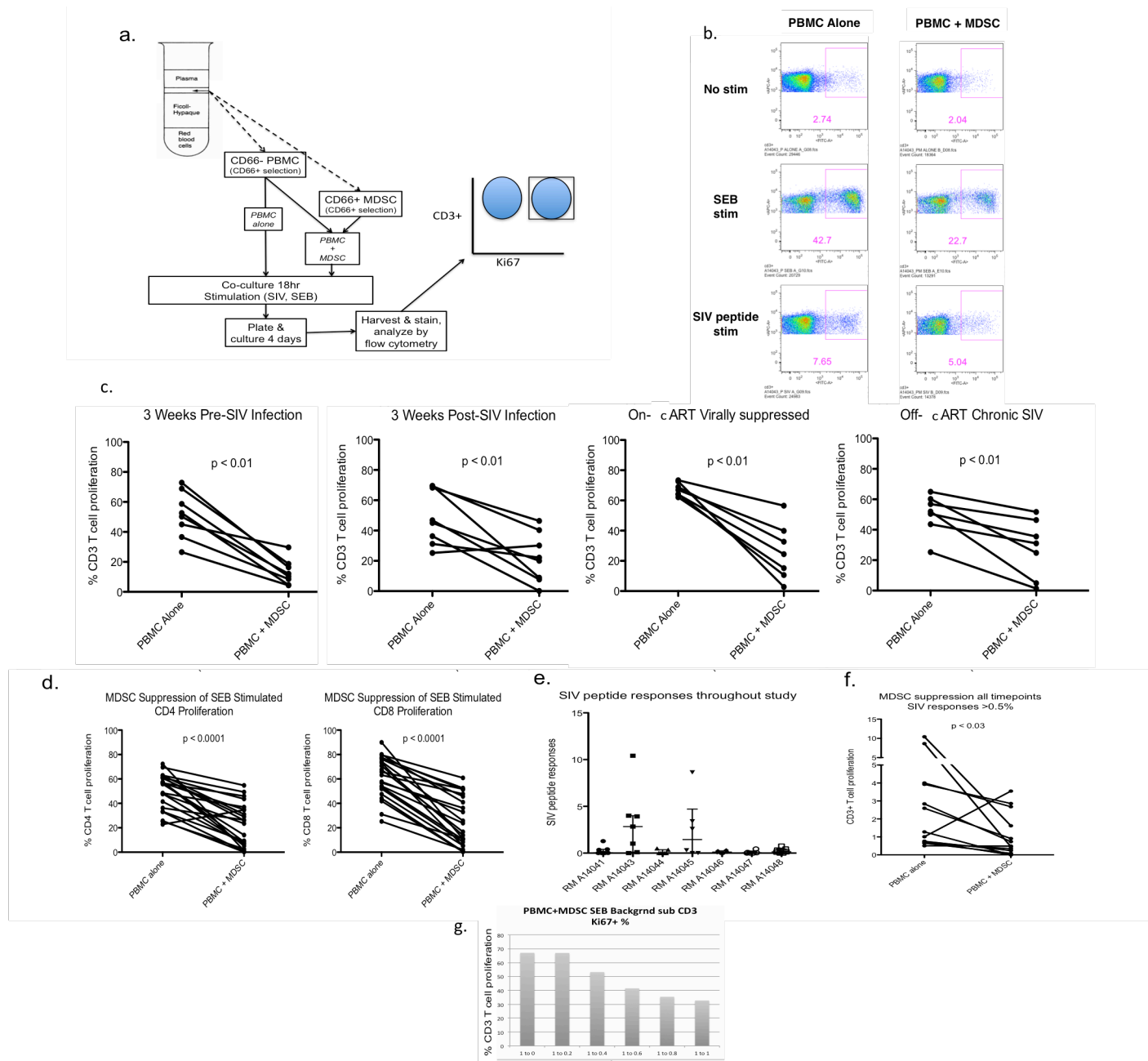


Figure 13. gMDSC suppress T cell proliferation at all stages of infection

CD66+ MDSC were depleted via magnetic bead separation from PBMC and cultured either alone or with CD66+ MDSC added back overnight, then stimulated with 1ug/ml 15mer SIVmac239 Gag peptide pool or 0.4ug/ml Staphylococcal enterotoxin B from *Staphylococcus aureus* for four days (A, F). Proliferation was measured by ICS for Ki67 (B). CD66+ MDSC-mediated suppression was measured by comparing the CD3 (C) CD4 and CD8 (D) proliferation stimulated in the absence and presence of 66+ cells. Total and median SIV Gag peptide responses were plotted for comparison (E). Dose response of MDSC was determined in five-day culture stimulated with SEB at various ratios (G). Proliferation levels were compared by Wilcoxon signed-rank test.

3.3 MDSC in lymphoid tissue exhibit suppressive function

Peripheral lymphoid organs were examined for MDSC infiltration at necropsy. We did not find elevated MDSC in lymph nodes when compared to MDSC levels in peripheral blood. However, there were elevated MDSC in the spleen that were comprised primarily of the granulocytic subset (Figure 14a). Suppressive function of gMDSC in the spleen was determined in one animal. We found MDSC suppression that was not observably different in the spleen vs. in the peripheral blood (Figure 14b).

3.4 Plasma cytokine levels correlate with MDSC

To determine if MDSC expansion was driven by inflammation during SIV infection plasma cytokine levels were measured by multiplex ELISA and compared to frequency of MDSC measured at the same time-points. At all data points collected there were direct and significant correlations, adjusted for multiple comparisons, with MDSC frequency and the systemic levels of inflammatory cytokines. IL-6 (Spearman $r=0.42$, $p=0.0003$), TNF α (Spearman $r=0.48$, $p<0.0001$), MIP-1 α (Spearman $r=0.47$, $p<0.0001$), MIF (Spearman $r=0.40$, $p=0.0005$), and IP-10 (Spearman $r=0.41$, $p=0.0004$) all correlated significantly with MDSC frequency (Table 2). We highlighted key cytokine kinetics including those of IL-6, TNF α , MIP-1 α , MIF, IP-10, VEGF and IL-1 β (Figure 15a). Correlations between many systemic inflammatory cytokines strengthened at time-points where the animals were not on suppressive therapy. During post-cART viremia, the association strengthened between MDSC frequency and TNF α (Spearman $r=0.68$, $p<0.0001$), MIP-1 α (Spearman $r=0.60$, $p=0.0003$), IL-6 (Spearman $r=0.58$, $p=0.0005$),

IL-1 β (Spearman $r=0.57$, $p=0.0007$), and MIP-1 β (Spearman $r=0.54$, $p=0.0014$) (Figure 15b). At time-points where viral load data was available, viral load trended toward correlating with MDSC frequency but did not reach statistical significance when adjusted for multiple analyses (Spearman $r=0.44$, $p=0.008^1$), and we observed stronger correlations between MDSC and the inflammatory cytokines listed above. Multivariate regression analysis with stepwise selection of the 29 cytokines assayed plus viral load data found MIF and TNF α to independently correlate with MDSC frequency ($r^2=0.30$, $p<0.05$) study-wide and TNF α to independently correlate in the post-cART viremic time-points ($r^2=0.42$, $p<0.05$).

¹ $p<0.0017$ considered significant

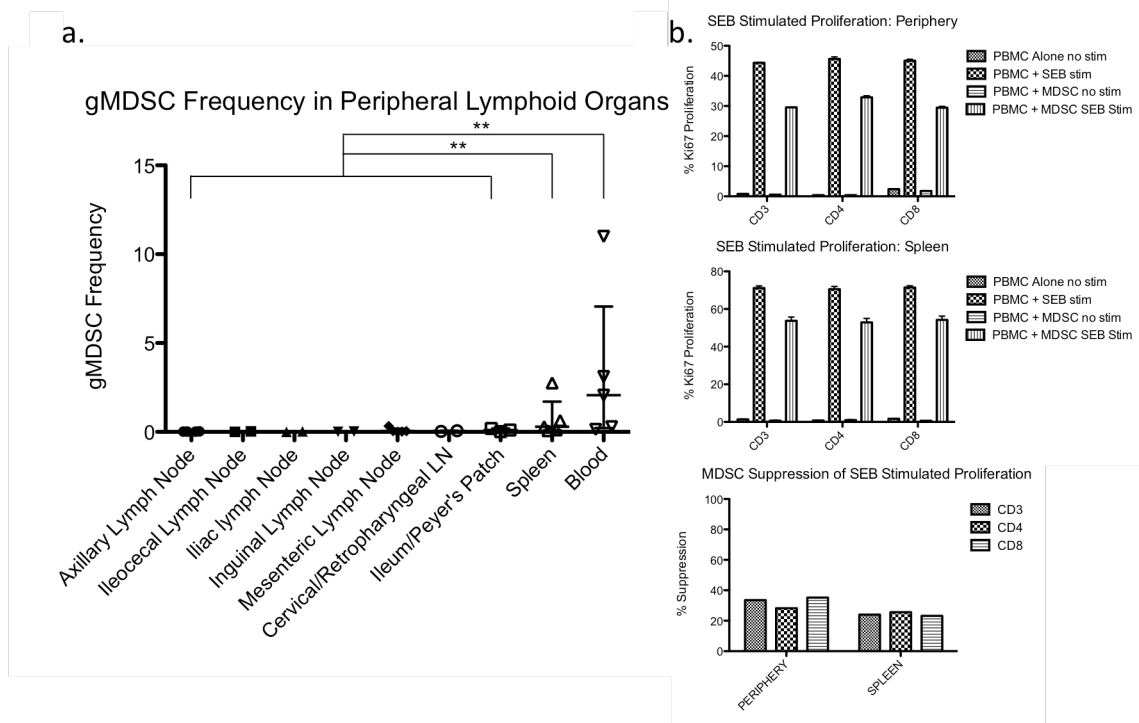


Figure 14. MDSC frequency in peripheral lymphoid organs

Peripheral lymphoid organs were excised at necropsy and examined for MDSC infiltration. Single-cell suspensions of ileum, spleen, and axillary, ileocecal, iliac, inguinal, mesenteric, cervical and retropharyngeal lymph nodes were density separated then stained for MDSC (A). gMDSC infiltration in lymph nodes, spleen and blood were compared (A). gMDSC suppressive function was determined in the spleen vs. the peripheral blood and no differences were observed (B). Median gMDSC frequencies were compared by Mann-Whitney U test.

Parameter: ALL TOTAL MDSC VS CYTOKINE PANEL	Number of XY Pairs	Spearman r	95% confidence interval	P value (two-tailed)	P value summary	Exact or approximate P value?	Is the correlation significant? (alpha=0.05)	Is the correlation significant adjusting for multiple tests? (adjusted alpha=0.0017)
MIP-1alpha (26)	73	0.4739	0.2673 to 0.6389	< 0.0001	****	Gaussian Approximation	Yes	Yes
TNF-alpha (52)	73	0.4834	0.2786 to 0.6461	< 0.0001	****	Gaussian Approximation	Yes	Yes
IL-6 (19)	73	0.4158	0.1987 to 0.5940	0.0003	***	Gaussian Approximation	Yes	Yes
IP-10 (56)	73	0.4061	0.1874 to 0.5864	0.0004	***	Gaussian Approximation	Yes	Yes
MIF (46)	73	0.3975	0.1776 to 0.5797	0.0005	***	Gaussian Approximation	Yes	Yes
IL-1beta (13)	73	0.348	0.1214 to 0.5402	0.0026	**	Gaussian Approximation	Yes	No
VEGF (36)	73	0.3255	0.09627 to 0.5220	0.005	**	Gaussian Approximation	Yes	No
IL-2 (54)	73	0.3164	0.08616 to 0.5145	0.0064	**	Gaussian Approximation	Yes	No
IL-4 (77)	73	-0.3065	-0.5065 to -0.07534	0.0083	**	Gaussian Approximation	Yes	No
MIP-1beta (28)	73	0.2905	0.05776 to 0.4932	0.0127	*	Gaussian Approximation	Yes	No
I-TAC (44)	73	0.2843	0.05111 to 0.4882	0.0148	*	Gaussian Approximation	Yes	No
IL-10 (15)	73	0.2674	0.03279 to 0.4741	0.0222	*	Gaussian Approximation	Yes	No
EGF (33)	73	0.2599	0.02475 to 0.4678	0.0264	*	Gaussian Approximation	Yes	No
IL-6 (78)	73	0.2505	0.01471 to 0.4599	0.0325	*	Gaussian Approximation	Yes	No
MCP-1 (29)	73	0.2504	0.01458 to 0.4598	0.0326	*	Gaussian Approximation	Yes	No
IL-1RA (51)	73	0.2114	-0.02665 to 0.4267	0.0727	ns	Gaussian Approximation	No	No
EOTAXIN (22)	73	0.2112	-0.02679 to 0.4266	0.0728	ns	Gaussian Approximation	No	No
IL-17 (25)	73	-0.1841	-0.4032 to 0.05500	0.119	ns	Gaussian Approximation	No	No
FGF-Basic (12)	73	0.1831	-0.05604 to 0.4023	0.1211	ns	Gaussian Approximation	No	No
GM-CSF (27)	73	-0.1694	-0.3904 to 0.07008	0.1519	ns	Gaussian Approximation	No	No
MDC (39)	73	0.145	-0.09492 to 0.3690	0.2209	ns	Gaussian Approximation	No	No
IL-5 (34)	73	-0.1274	-0.3534 to 0.1127	0.2829	ns	Gaussian Approximation	No	No
IL-15 (30)	73	-0.103	-0.3316 to 0.1371	0.3861	ns	Gaussian Approximation	No	No
G-CSF (14)	73	0.08559	-0.1542 to 0.3159	0.4715	ns	Gaussian Approximation	No	No
HGF (35)	73	0.07521	-0.1644 to 0.3064	0.5271	ns	Gaussian Approximation	No	No
RANTES (21)	73	-0.07173	-0.3033 to 0.1678	0.5465	ns	Gaussian Approximation	No	No
MIG (63)	73	0.05932	-0.1799 to 0.2919	0.6181	ns	Gaussian Approximation	No	No
IFNgamma (38)	73	0.04994	-0.1890 to 0.2833	0.6748	ns	Gaussian Approximation	No	No
IL-12 (20)	73	0.04723	-0.1916 to 0.2808	0.6915	ns	Gaussian Approximation	No	No

Table 2. Plasma cytokine levels correlated with MDSC frequency

Plasma was stored at -80°C and batch tested as per kit instructions using the Monkey Cytokine Magnetic 29-Plex Panel for GM-CSF, TNF- α , IL-1 β , IL-4, IL-6, MIG, VEGF, HGF, EGF, IL-8, IL-17, MIP-1 α , IL-12, IL-10, FGF-Basic, IFN- γ , G-CSF, MCP-1, IL-15, IP-10, MIP-1 β , Eotaxin, RANTES, IL-1RA, I-TAC, MDC, IL-5, IL-2, and MIF at weeks -3, 3, 10, 14, 18, 37, 40, 46, 56 and 68. MDSC frequencies were correlated to cytokine levels by Spearman's rank correlation coefficient. P values less than 0.0017 were considered significant.

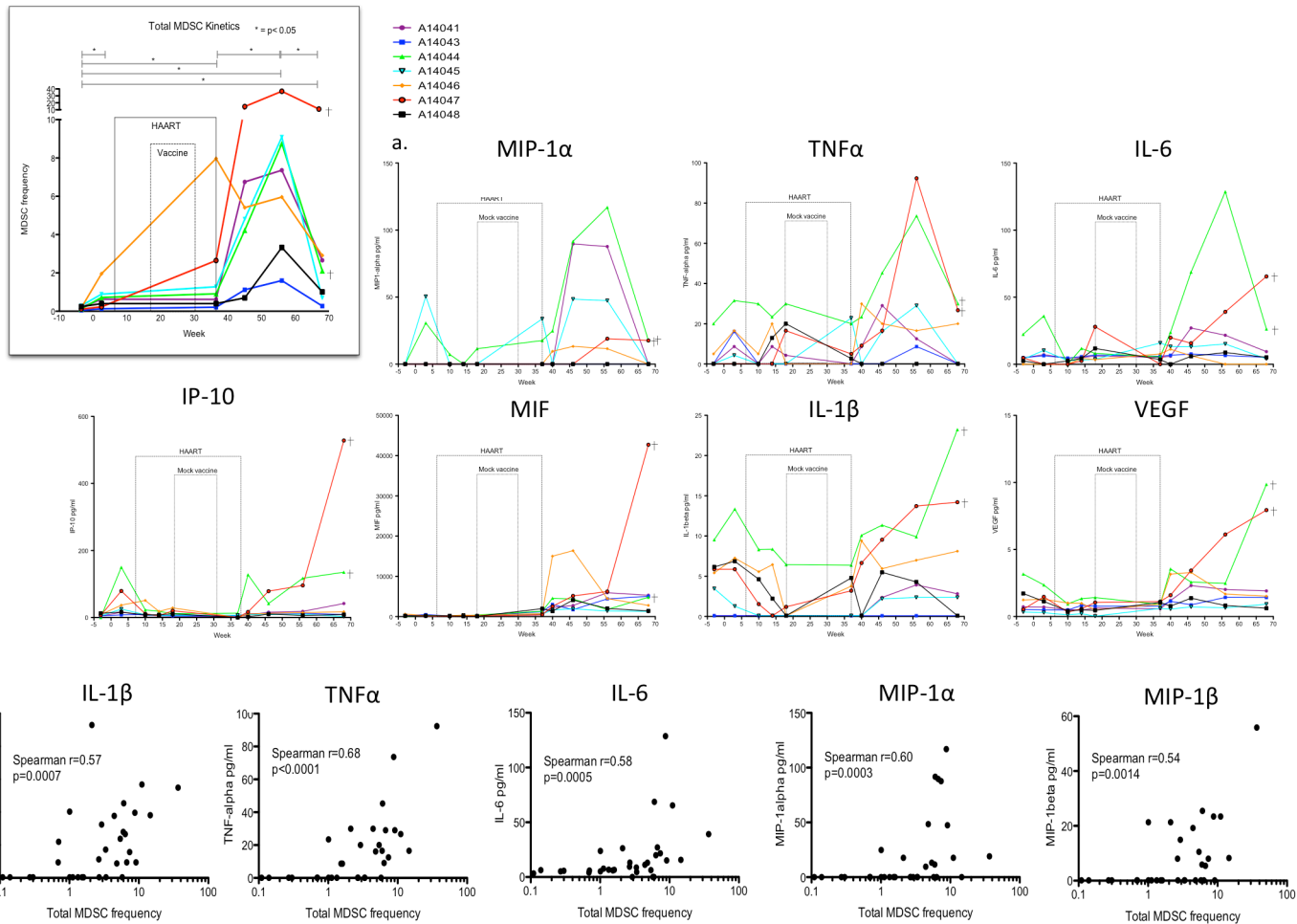


Figure 15. Plasma cytokine levels over course of SIV infection

Plasma was stored at -80°C and batch tested as per kit instructions using the Monkey Cytokine Magnetic 29-Plex Panel for GM-CSF, TNF- α , IL-1 β , IL-4, IL-6, MIG, VEGF, HGF, EGF, IL-8, IL-17, MIP-1 α , IL-12, IL-10, FGF-Basic, IFN- γ , G-CSF, MCP-1, IL-15, IP-10, MIP-1 β , Eotaxin, RANTES, IL-1RA, I-TAC, MDC, IL-5, IL-2, and MIF at weeks -3, 3, 10, 14, 18, 37, 40, 46, 56 and 68. Cytokine kinetics are shown for MIP-1 α & β , TNF α , IL-6, IP-10, MIF, IL-1 β , and VEGF which significantly correlated or trended with MDSC frequency study wide (A). During post-cART viremia correlations between MDSC and TNF α , MIP-1 α & β , IL-6, IL-1 β strengthened (B). MDSC frequencies were correlated to cytokine levels by Spearman's rank correlation coefficient.

3.5 MDSC frequency pre-SIV correlates with set-point viral load

We measured MDSC frequencies pre-SIV infection in two additional cohorts of animals. One group of five animals (Cohort 2) had aberrantly high MDSC frequencies pre-SIV infection. The median pre-SIV frequency in this group was 5.67% compared to 0.15% and 0.46% in cohorts 1 and 3, respectively (Figure 16a). We used this aberrant cohort to determine if elevated MDSC frequency pre-SIV infection could affect disease progression by decreasing activated target cells (thereby decreasing disease severity or progression) or by suppressing early immune response (thereby increasing disease severity or progression). A positive correlation was found between set-point viral load and MDSC frequency in this cohort (Figure 16b). The granulocytic subset of MDSC strongly correlated with viral load (Spearman $r=1.00$, $p=0.017$) while the monocytic subset did not (Spearman $r=0.30$, $p=0.68$) (Figure 16b). We analyzed the baseline cytokine levels between the two cohorts but did not find significant differences when adjusting for multiple tests (data not shown). Trends were found with MIP-1 α and IL-6 (Mann Whitney test $p<0.03$, $p=0.07$, respectively) and while MIP-1 α correlated directly with gMDSC frequency (Spearman $r=0.66$, $p=0.02$), IL-6 did not (Spearman $r=0.38$, $p=0.22$) (data not shown).

3.6 MDSC are not induced in culture by SIV

We have demonstrated that the increased levels of certain pro-inflammatory cytokines strongly correlate to the frequencies of gMDSC. These cytokines may be the drivers of increased MDSC frequency. However, we sought to understand if viral

particles would also play a role based on previous studies. Garg et al. showed that the monocytic subset of MDSC can be induced in a five day culture with heat-killed virus and the HIV viral protein GP120 alone [38], and *in vivo*, animals that received the SIV vaccine had worse virologic control compared to adjuvant alone animals, suggesting MDSC were elicited by viral peptides and hampered immune control of SIV [42]. Therefore, we sought to understand if gMDSC and mMDSC are inducible in our model by virus or viral products. Co-culture of uninfected rhesus macaque PBMC with SIV peptide pools, heat killed and live virus at two different concentrations failed to induce an increase in gMDSC and mMDSC in our experiments (Figure 17).

3.7 Soluble CD14 levels elevated post-cART

Levels of sCD14 in circulating plasma were determined at study weeks 0-40 off-site by sCD14 ELISA. Levels of sCD14 were significantly higher during the post-cART viremia ($p < 0.001$) compared to levels during acute infection (Figure 18a). Levels of sCD14 increased incrementally throughout the study, despite cART therapy (Figure 18b).

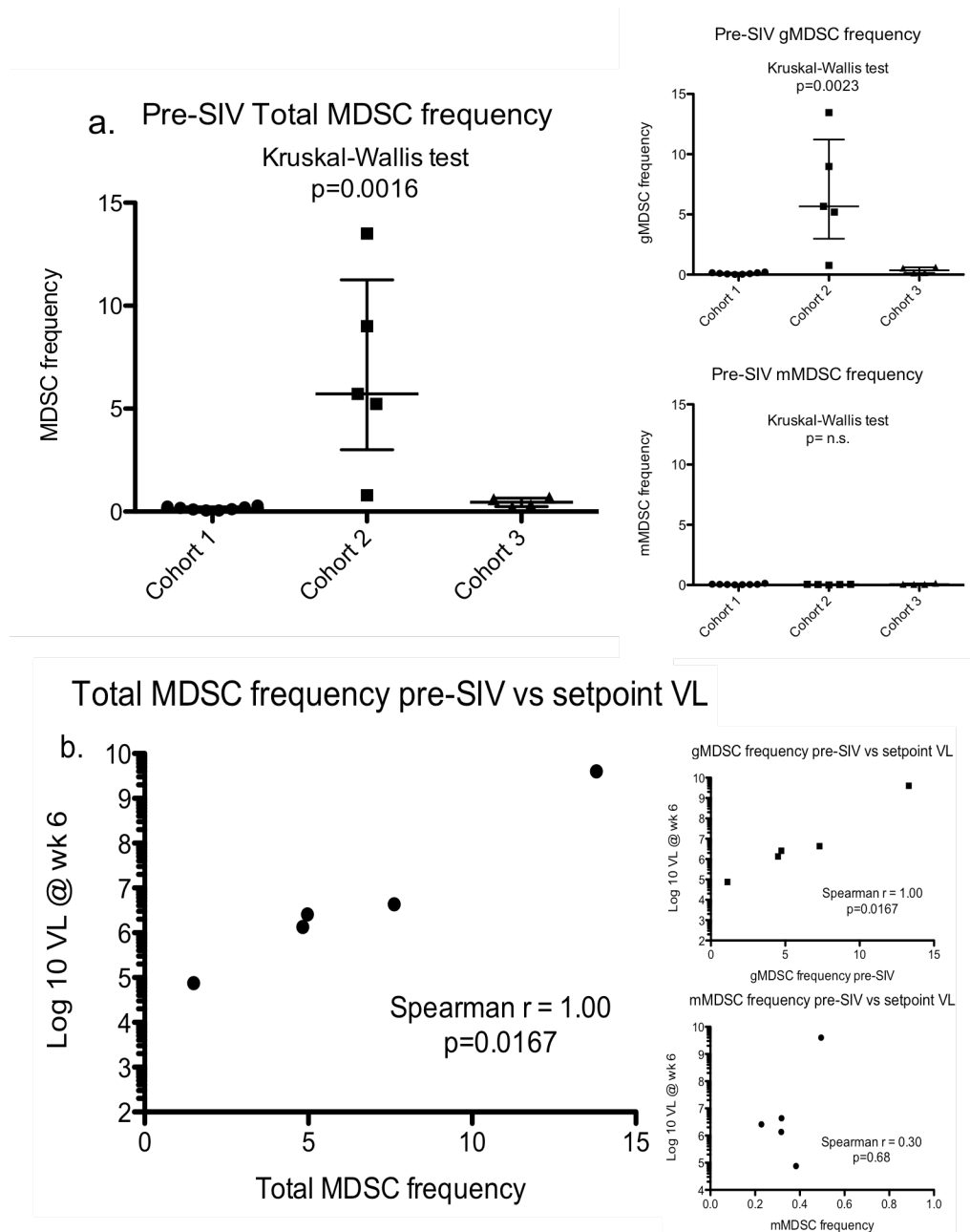


Figure 16. MDSC frequency pre-infection correlates with higher viral loads

Baseline frequency of MDSC were determined for Cohort 1 -2 at four and three weeks pre-SIV infection and averaged while Cohort 3 was assessed at one time-point (four weeks pre-SIV infection). Baseline MDSC frequency in all cohorts were compared by Kruskal-Wallis test (A). Set point VL was correlated with MDSC frequency in Cohort 2 by Spearman's rank correlation coefficient. (B).

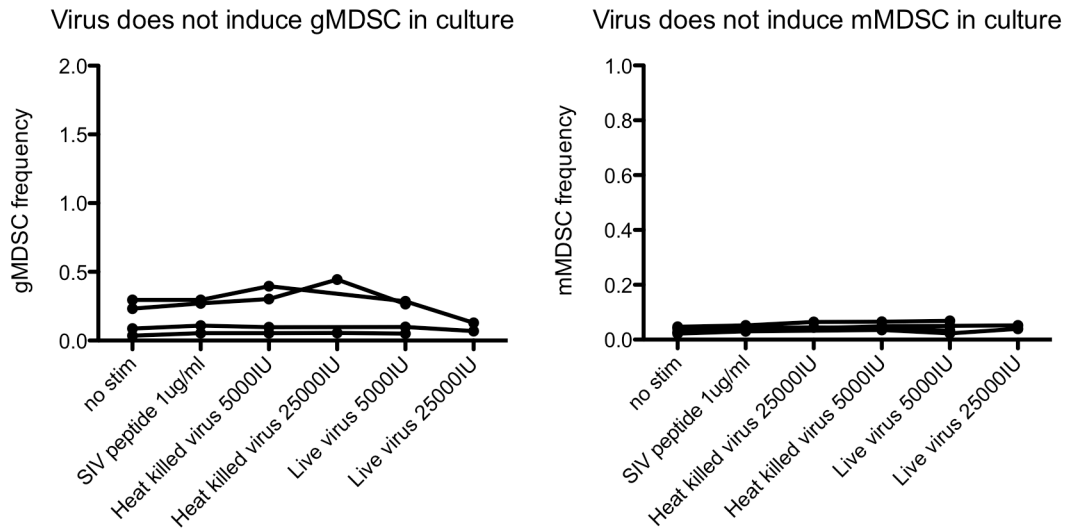


Figure 17. SIV does not induce MDSC in culture

1×10^6 PBMC from four SIV-uninfected rhesus macaques were cultured for five days either alone or with 1ug/ml SIV Gag peptide pool, heat killed or live SIV/DeltaB670 virus at approximately 5,000 and 25,000IU. MDSC frequency was assessed and plotted for each animal.

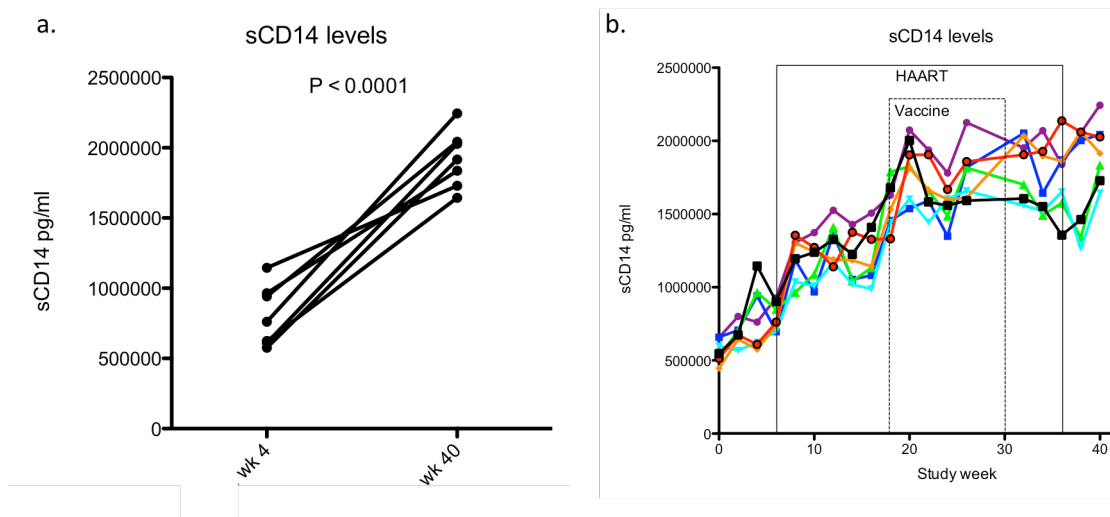


Figure 18. Levels of sCD14 elevated during post-cART viremia

Soluble CD14 levels in circulating plasma were determined at study weeks 0-40 off-site by sCD14 ELISA. Levels of sCD14 were significantly higher during the post-cART viremia (at study week 40, 3 weeks post-cART) compared to levels during acute infection (at study week 4, 4 weeks post-infection) (A). Levels of sCD14 increased incrementally throughout the study, despite cART therapy (B). Week 4 vs. week 40 sCD14 levels compared by Wilcoxon signed-rank test.

3.8 Discussion of MDSC kinetics during SIV infection

Longitudinal analyses of MDSC kinetics showed that the frequency of MDSC was low pre-SIV infection as expected for otherwise healthy animals. MDSC frequency increased slightly, yet significantly, during acute SIV infection and was sustained even during effective cART. In the 20 weeks post-cART MDSC frequency increased markedly, though transiently, for most animals. Of note, two of the three animals with the highest peak MDSC frequencies were euthanized with AIDS-defining illnesses before end-of-study. Although we observed a correlation between the gMDSC subset at week 12 post infection and set point viral load in the pilot study, we did not observe strong correlations between set point viral load and MDSC frequency in the longitudinal study (data not shown). This difference is likely attributable to the addition of cART at week 6 in the longitudinal study, whereas in the pilot study, MDSC frequency was obtained 12 weeks post-infection in the absence of viral suppression.

The granulocytic fraction of MDSC was the driver of the elevated MDSC observed study-wide, thus functional characterization focused on this subset. We used either the superantigen Staphylococcal enterotoxin B (SEB) or a SIV Gag peptide pool to stimulate T cell proliferation. Granulocytic MDSC were able to suppress SEB-stimulated T cell proliferation quite consistently at all study time-points assayed and suppressed both CD4 and CD8 T cell proliferation in a dose-dependent manner. SIV peptide responses were more variable than the polyclonal SEB stimulus, but for SIV responses over 0.5% we observed suppression by MDSC. Anecdotally, the two animals with the highest SIV peptide responses over the course of the study also had the lower median MDSC frequencies over the course of the study. It is possible that MDSC in the other animals

early in infection hindered the development of strong SIV responses, as MDSC hinder the migration of naïve T cells to peripheral lymphoid organs via cleavage of CD62L from the cell surface.

We observed some MDSC infiltration in the spleen but not in any other peripheral lymphoid organs at necropsy. We did not assay peripheral lymphoid organs during the times of peak MDSC elevation and only examined these sites at necropsy. This may have decreased our ability to detect infiltration or caused us to miss times of infection where MDSC might be more likely to traffic to lymphoid tissues (during the acute phase or in the highly inflammatory 20 weeks post-cART interruption), as MDSC levels had declined by end-of-study necropsy. The splenic MDSC population has been described by others in the mouse tumor model (reviewed in [88]). Splenic MDSCs have been reported to be less suppressive than those at the tumor site; however, in our study similar suppressive ability of MDSC was found for the two sites when assessing T cell proliferation in response to SEB. The disagreement of these results may be due to the hypoxic and inflammatory nature of the tumor site in cancer. While there is no reason to think that MDSC in peripheral blood during chronic viral infection would be differentially activated by circulating elevated inflammatory cytokines compared to MDSC in the spleen, the hypoxia and inflammation at the tumor site has been shown to induce suppressive effects of MDSC that do not extend to the periphery [1].

Levels of cytokines that associated with MDSC frequency over the course of the study were IL-6, TNF α , MIP-1 α , MIF, VEGF and IP-10 and the peak cytokine levels were achieved 10-30 weeks post-cART interruption for most. During the marked increase in cytokines post-cART MDSC frequency strongly associated with elevations in IL-6,

TNF α , IL-1 β , MIP-1 α and MIP-1 β , and these associations were stronger than the association between viral load and MDSC frequency. The initial viremia pre-antiretroviral therapy did not induce the same high levels of cytokines and MDSC seen after treatment interruption despite similar set points, suggesting viral load alone is not the driving force of this phenomenon. IL-6 and IL-1 β are well known to activate and expand MDSC in mouse tumor models [2]. Macrophage Inflammatory Protein 1 α , or MIP-1 α , is known to recruit and activate granulocytes [89]. Neutrophils express IL-1R1, the receptor for IL-1 β and also express the receptors for MIP-1 α , IL-1 β , IL-6, and the TNF α receptor CD120b [7]. Multivariate regression analysis with stepwise selection of the 29 cytokines assayed plus viral load data found MIF and TNF α to independently correlate with MDSC frequency. MIF (macrophage migration inhibitory factor) is an inflammatory cytokine elevated in cancer and sepsis that has been shown to induce MDSC of the monocytic subset and enhance tumor progression [90] while inhibition of MIF can change mMDSCs to a non-suppressive monocytic phenotype [91]. TNF signaling is known to drive MDSC in the mouse cancer model. TNF-receptor deficient mice exhibit decreased MDSC frequencies caused by decreased MDSC survival [92]. In HIV+ individuals with evidence of microbial translocation MIF levels have been found to be elevated compared to healthy controls [93]. As MIF is released in response to LPS [94], it is reasonable to hypothesize that SIV-infection induced microbial translocation is playing a role in the generation of MDSC in our model. TNF α is known to disrupt epithelial tight junctions and antibody against TNF α reduces this disruption [95]. As MIF can also drive TNF α production, and large amounts of TNF can be secreted by MDSC, we envision in viremic infection a feedback loop is generated where MIF and TNF α both

directly and indirectly induce MDSC with major contributions by microbial translocation, viral particles and additional inflammatory cytokines. Progressive increases in microbial products or a secondary microbial translocation event is likely driving the transient cytokine storm and MDSC surge observed post-cART. Indeed when we tested for sCD14 we found marked elevations during the post cART viremia compared to acute viremia (Figure 18).

Our results add to the body of work describing MDSC frequency and function in chronic retroviral infections and identify a novel, transiently elevated population of gMDSC subsequent to cART treatment interruption. Plasma cytokine measurements suggest microbial translocation is the driving force of this population. Limitations of this work were the small specimen volume received at each time-point and the requirement of demonstration of suppressive ability to define a population of MDSC. This resulted in our prioritizing frequency measurements and characterization of suppressive function rather than mechanistic experiments over the course of the study. Based on the cytokine elevations characteristic of microbial translocation, experimental determination of the effect of TNF α blockade during cART treatment interruption to enhance tight junction stability and potentially reduce the inflammatory cytokine storm may be warranted.

Chapter 4: Final discussion

4.0 Discussion

Several lines of evidence suggest MDSC are playing a role in the immune suppression observed in chronic retroviral infection. MDSC have been found to suppress T cell function in many populations of retroviral-infected humans and animals [35-39, 41, 42]. MDSC are more frequent in untreated infection than during cART [35, 37], and less frequent with higher CD4 counts [35, 37]. However, during retroviral infection it has not been clear which subset, granulocytic or monocytic, is more relevant. Differences among the studies in HIV+ humans that may have led to the disparate results include differences in the health/disease stage of HIV+ participants among the studies.

Groups reporting elevation of mMDSC examined HIV- infected individuals with low CD4 counts and at advanced clinical stage [37, 38]. The majority of these HIV+ individuals in Qin et al.'s study (~70%) had very low CD4 counts (<200) with less than 10% of the population having a CD4 count above 350. The majority of participants (~70%) were also CDC classification C HIV clinical stage (experiencing AIDS-symptoms). Similarly, the HIV+ population studied by Garg et al. had a low median CD4 count (below 200), and characterization of mMDSC expansion was performed *ex vivo*. As for the studies where gMDSC were found to be elevated, the CD4 counts of both groups' enrolled HIV+ participants were higher. For example, Vollbrecht et al. reported an average CD4 count of 422 (range: 16-1,237) and Bowers et al. reported a median CD4+ T cell count of 444 (range: 102-1,385) not on therapy and a median CD4+ T cell count of 657 (range: 189-1,763) on therapy [35, 36]. In our studies, the granulocytic subset of MDSC was the most compelling in chronic HIV infection and over the course

of SIV infection, while the monocytic subset was infrequent in chronic HIV infection and only significantly increased in SIV infection at week 56, during the post-cART cytokine elevation.

These observations along with data in the reviewed literature fit with a theory whereby granulocytic MDSC accumulate over time during chronic retroviral infection in otherwise healthy individuals while expansion of the monocytic subset only occurs during periods of poor health or in individuals who are in poor health. One caveat to this theory is that as week 56 also saw peak gMDSC frequencies comprising 93% of the total population, and in the pilot study gMDSC comprised a median 74% of the MDSC population at week 12, this theory does not completely explain why Qin et al did not find a functional and frequent granulocytic MDSC subset in their study.

In the reviewed literature and in our studies there is no consensus as to the mechanism(s) utilized by MDSC induced during retroviral infection. We observed an arginine-insensitive but contact or microenvironment dependent suppression of T cell proliferation in the HIV+ individuals studied. Arginase-1 is a well-described inhibitor of T cell function by the granulocytic subset of MDSC, however when cultures were supplemented with 10x the physiologic level of arginine to rescue proliferative ability we observed no difference in suppression. This suggests arginase-1 may not be playing a role in the T cell suppression we observed. As arginase-1 depletes arginine in the microenvironment leading to loss of CD3 ζ , and iNOS utilizes arginine to create nitric oxide, the insensitivity of gMDSC to arginine-rescue in 2 independent donors and experiments suggests neither mechanism is critical to the suppression observed. We have not yet examined the effects of MDSC-mediated cysteine restriction as this mechanism

has only been described in bulk mouse MDSC (Gr1 antibody, which does not differentiate gMDSC /mMDSC subset) and has yet to be observed in humans. We suspect reactive oxygen species are playing a role in the suppressive mechanism, as these are canonically generated by neutrophils to kill phagocytosed bacteria. Also, ROS are by name reactive and thus short-lived, supporting our transwell® data of contact dependence. ROS-inhibition experiments were inconclusive as in the individuals tested there was no suppression observed of polyclonal stimulus and no HIV Gag response above background in control wells (data not shown).

The lack of consistency in T cell responses and in MDSC-mediated suppression in our human study was not uncommon and led to the optimized experiments in the rhesus macaque model. In this model we observed more consistent responses to stimuli, as well as consistent MDSC-mediated suppression of responses. However, as we obtained these specimens from an ongoing study we did not have the ability to test MDSC-modifying compounds *in vivo* or have sufficient sample to explore questions regarding mechanism of action *ex vivo*.

Several *in vitro* studies in cancer mouse models have disagreed whether the granulocytic subset of MDSC is less suppressive than the monocytic subset with observations of similar suppressive ability [96] and of decreased suppressive ability in gMDSC [97]. In our study of SIV-infected rhesus macaques, we observed potent suppressive effects of the granulocytic subset of MDSC in low-arginine media. As the suppression of MDSC in the mouse model was determined *in vitro* using traditional culture media which has 10x physiologic levels of arginine and monocytic MDSC primarily utilize iNOS to exert suppressive function via metabolism of arginine to

citrulline and NO, the results suggesting mMDSC are more suppressive may have been a laboratory or experimental artifact. mMDSC may utilize the overabundance of arginine in media to metabolize copious amounts of NO while the gMDSC arginase-1 may not be able to overcome the abundance of arginine in culture and thus appear to have less suppressive ability.

In the cancer field it has been suggested that MDSC suppression can be site-specific and limited to the location of the tumor. Whether MDSC in retroviral infections also home to discrete sites of increased inflammation was not addressed by these studies. As the specific location(s) of the reservoir(s) of HIV persistence are as yet uncharacterized, it is possible that increased inflammation and low level replication of virus at these sites attract MDSC and create a tumor-like suppressive environment. These MDSC, if present at sites of replication, may suppress HIV/SIV specific T cell responses to viral peptides, permitting persistence.

4.1 Summary

In summary, this work has characterized the frequency and function of the MDSC population in chronic retroviral infection. gMDSC accumulate during acute infection and remain elevated even on suppressive cART, and can suppress HIV T cell responses. In addition, we have identified two as yet unidentified periods during chronic retroviral infection where MDSC are significantly elevated: in an aging host on suppressive cART, and in a previously virally suppressed host post treatment interruption (Figure 19). These elevated MDSC correlate with inflammatory cytokines indicative of microbial

translocation. These novel findings suggest there may be a role for investigating therapies such as anti-TNF α to reduce gastrointestinal epithelial barrier disruption at these times.

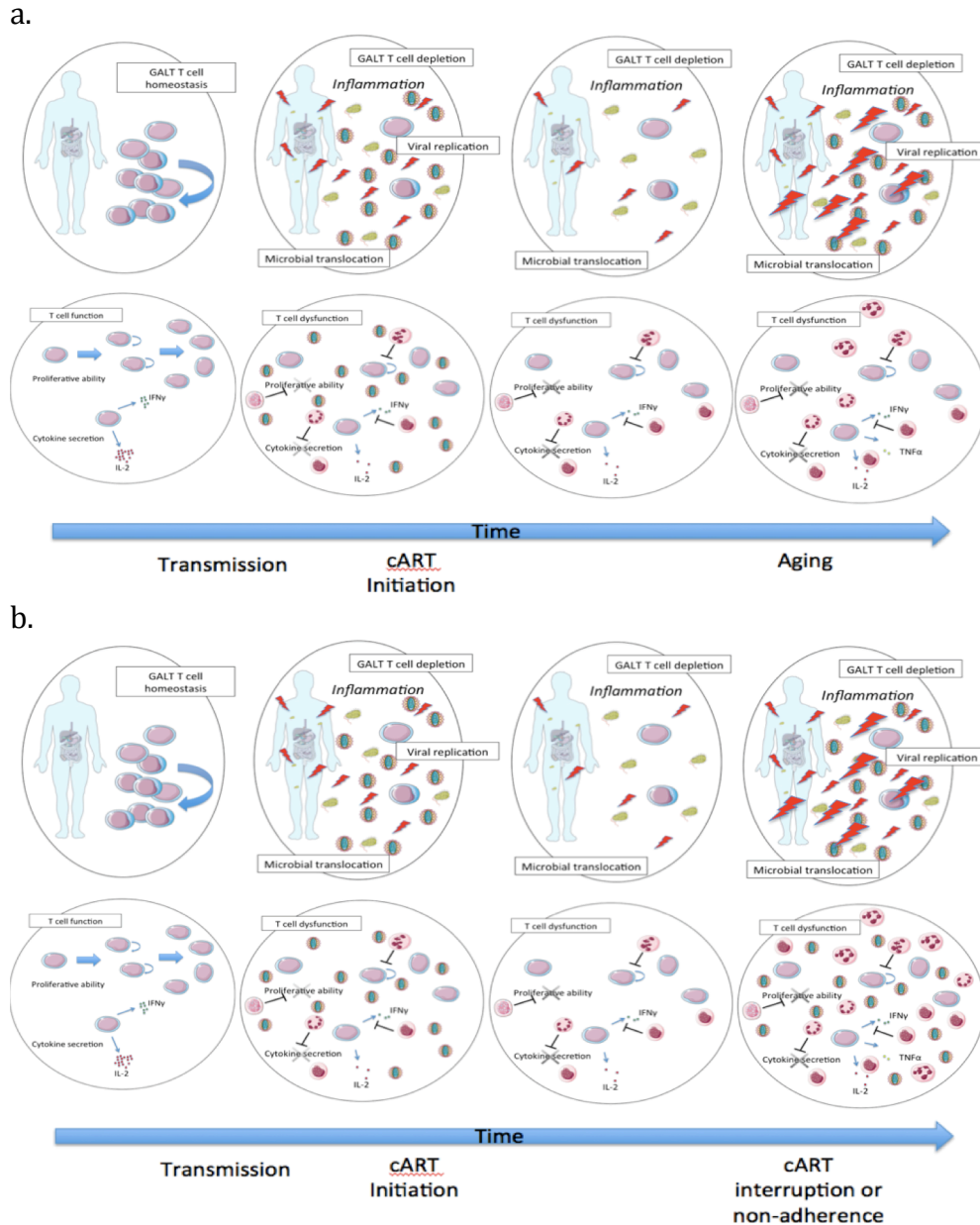


Figure 19. Model of MDSC in retroviral infection

We characterized MDSC in retroviral-infected hosts over a spectrum of ages and longitudinally and observed accumulation of suppressive gMDSC. These gMDSC suppress virus-specific T cell responses at all stages of infection. We identified two distinct times of elevated inflammation in chronic retroviral infection where there is a marked elevation of MDSC. MDSC are elevated during aging in an antiretroviral-treated host (A) and MDSC are elevated post-cART treatment interruption in a previously virally suppressed host (B). These elevated MDSC correlate with inflammatory cytokines indicative of microbial translocation. These novel findings suggest there may be a role for investigating therapies such as anti-TNF α to reduce gastrointestinal epithelial barrier disruption at these times and increase T cell function by reducing MDSC frequencies.

4.2 Further questions

As blood cannot be frozen previous to functional or even frequency analyses of the MDSC population, our analyses were limited to the populations we had immediate access to. This population includes the HIV+ population in Seattle, WA and the rhesus macaque (*Macaca mulatta*) control cohort of a therapeutic vaccine trial. This limitation precluded our answering additional questions including addressing the differences we observed in MDSC frequency by gender and by cohort as well as teasing out the mechanism of action.

The animal work comprised 100% male animals and while human enrollment and recruiting in Seattle was not restricted based on gender, we were able to obtain specimens from 40% male HIV- individuals and 90% male HIV+ individuals. We observed elevated frequencies across all ages in women in our human work and chose to limit the majority of our analyses to men, who comprised the majority of the HIV+ population, as we were concerned the gender differences between HIV- and HIV+ populations would confound the results. Although in our human work we chose to focus our analyses on men who comprised the majority of HIV+ subjects, we remain interested in what factors are driving these differences in MDSC frequency, and potentially function, between men and women.

The mMDSC subset of MDSC are elevated in human pregnancy. These MDSC are inducible by estradiol (but not progesterone) resulting in downstream S100A8 and S100A9 expression and ROS production. MDSC express estradiol receptor (ER) alpha and administration of estradiol resulted in higher phosphorylated STAT3, the main transcription factor driving MDSC expansion and activation [98]. Our group has

observed a population of gMDSC that is elevated in pregnant women and their neonates [99]. Whether these gMDSC are estradiol-induced, and whether a similar population of gMDSC are inducible by estradiol in non-pregnant women, remains to be seen. We observed MDSC increase at all age groups, including those over 60 years old, and post-menopausal women have similar levels of estradiol and had similar, if a little higher, median ages as men (women: median age 79, range 65-92, men: median age 74, range 65-83). As in this older group the women are most likely post-menopausal, this suggests hormones may be playing a role but are not the only driver of the difference in MDSC between genders.

Another difference between men and women is HIV disease progression which is more rapid in women, despite having higher CD4 cell counts and up to 40% lower viral loads than men. Plasmacytoid dendritic cell (pDC) sensing of HIV through toll-like receptor 7 (TLR7) leads to higher production of IFN α and, in fact, estradiol is implicated in sensitizing these pDCs to TLR7 stimulus. One downstream effect of elevated IFN α is a higher response during acute infection leading to better viral control by increasing interferon-stimulated genes. Another downstream effect is that later in infection there is worse chronic inflammation and immune activation by the same interferon stimulated genes [100]. Therefore, it is plausible that elevation of MDSC in women is driven by the downstream effects of pDC estradiol sensitization to TLR7 stimulus which is evident in HIV infection but also applicable to other infections. Although our population of HIV+, cART suppressed individuals consisted primarily of men, women comprise the majority of the infected population in sub-Saharan Africa, the region of greatest importance and incidence. Unfortunately by focusing our results on men we are participating in a long-

standing tradition: in half of the phase 2-3 HIV vaccine trials of late, >94% of participants were male [100].

Another unanswered question is the reason for the aberrant elevation of MDSC in Cohort 2 pre-SIV infection compared to two other healthy cohorts of animals. This cohort did not come from a different source population of animals or have health metrics indicating they were otherwise abnormal. Interestingly, these animals were slightly older (4-5 years of age) than the animals we followed in Cohort 1 (three to four years of age). When we correlated starting MDSC frequency with age we found a significant correlation (Spearman $r=0.76$, $p<0.01$, data not shown). As rhesus macaques live to about 25 years of age, ‘aging’ is not likely to have caused the frequency expansion. Rhesus macaque males reach puberty around age 3 and are sexually mature around age 4. As there is a possible hormonal component to the generation of MDSC, it would be interesting to further investigate whether there is a transient elevation of MDSC in puberty.

Limitations of this work include variability in suppression observed in the human data and the small specimen volume received at each time-point from the rhesus macaques. Because demonstration of suppressive ability is imperative to define MDSC, we prioritized frequency measurements and characterization of suppressive function over the course of the study. This limited our ability to conduct mechanistic experiments in the rhesus macaque model. Our human data suggests while contact or proximity is playing a role in the T cell suppression observed, arginase-1 may not be a key player. Further studies are needed to determine the effect of inhibitors of known mechanisms of MDSC

suppression in this model including inhibitors of Arginase-1 and ROS to investigate mechanism of action.

Lastly, plasma cytokine measurements suggested microbial translocation is the driving force of this population. We observed a marked increase in sCD14 between acute and post-cART viremia despite similar levels of virus. This recent finding needs to be confirmed with measurement of LPS-binding protein (LBP). This is important because while CD14 is the receptor for LPS, measurement of sCD14 is not completely specific for microbial translocation. Increasing sCD14 indicates LPS is likely present but sCD14 can also rise during increased monocyte activation.

4.3 Concluding statement and implications

Our results add to the body of work characterizing MDSC frequency and function in chronic retroviral infections in a wide spectrum of ages. We also identified a novel, transiently elevated population of gMDSC correlating with large increases in inflammatory cytokines subsequent to cART treatment interruption. The initial viremia and post-cART viremia were similar in magnitude however there was not similar induction of inflammatory cytokine and MDSC in relation to virus. The US Department of Health and Human Services recommendations have changed to start all HIV+ individuals in the United States on antiretroviral therapy regardless of CD4 count based on data from the START and TEMPRANO studies [101]. Therefore, this work highlights the importance of continued adherence in these populations. Future work examining the role of FDA-approved therapies that abrogate microbial translocation or disable MDSC suppression in retroviral infection may be warranted.

Methods

Cross-sectional MDSC characterization in HIV infection

Specimen collection

HIV+ participants were enrolled at the Harborview Madison Clinic (Seattle, WA) while HIV- participants were enrolled at the Seattle BioMed Blood Draw Program and University of Washington (Seattle, WA). HIV+ individuals who have been seropositive for at least five years, on antiretroviral therapy and virally suppressed for at least one year were enrolled. Blood was collected in sodium heparin tubes and transported for immediate processing. Plasma was separated for 20 minutes at 2000rpm then frozen in 500ul aliquots at -80°C. Blood was then diluted to 25ml with PBS (Mediatech Inc) and overlaid on 15ml Ficoll-Paque PREMIUM (GE Healthcare) and spun for 20 minutes at 2000rpm. PBMC were removed and rinsed with 50ml PBS and resuspended at 1×10^8 cells/ml in EasySep™ Buffer (Stemcell Technologies).

MDSC frequency determination

Cells were stained for MDSC frequency with the following panel: CD11b PeCy7 (Miltenyi Biotec), CD14 PE (Becton Dickinson), CD15 APC (Becton Dickinson), CD33 PE-Cy5 (Becton Dickinson), and HLA-DR APC-Cy7 (Fisher Scientific). Gating was determined by fluorescence minus one (FMO) and compensation control values.

MDSC depletion and functional experiments

CD15+ myeloid-derived suppressor cells were separated from half of total PBMC, as per kit instructions using CD15 magnetic bead isolation (EasySep™). CD15 depleted PBMC or undepleted PBMC were stimulated with 2ug/ml pooled HIV Gag 15mer overlapping peptides (NIH AIDS Research & Reagent Program), 2ug/ml CMV pp65 peptide pool (NIH AIDS Research & Reagent Program), 10ul/ml Dynabeads CD3/28 CTS™ (Life Technologies), 0.4ug/ml Staphylococcal enterotoxin B from *Staphylococcus aureus* (Sigma Aldrich) or 2ug/ml phytohemagglutinin (PHA; Remel) then cultured at 37°C, 5% CO₂, for five days. Duplicate control unstimulated wells for each cell mixture were included for background proliferation subtraction. Experimental results with background proliferation higher than 5% were discarded. Proliferation was measured by ICS for Ki67 Alexa Fluor 488 (Becton Dickinson) and by CellTrace™ CFSE (Molecular Probes™). CD15+ MDSC mediated suppression was measured by comparing the proliferation stimulated in the absence of CD15+ cells with the proliferation stimulated in the presence of CD15+ MDSC. Viability in culture was determined by time course with Live Dead Aqua (Thermo Fisher).

Mechanistic experiments

All experiments were cultured for five days in custom arginine-low media: SILAC media (Sigma Aldrich) plus filter-sterilized L-arginine monohydrochloride (0.115mM, Sigma Aldrich) and filter-sterilized L-lysine hydrochloride (0.2186mM, Sigma Aldrich), 15% human serum (Sigma Aldrich), Penicillin-Streptomycin-Glutamine (0.5mg/ml, Thermo Fisher). Arginine rescue experiments were performed in 1.15mM L-arginine monohydrochloride (Sigma Aldrich). Inhibition of arginase-1 by nor-NOHA

acetate (Enzo Life Sciences) and ROS by ROS inhibitor YCG063 (Calbiochem) were tested in custom low-arginine media as above.

Contact dependence

Contact and microenvironment dependence experiments utilized Transwell® Permeable Supports (Corning). Experiments were performed as above; however, all PBMC were depleted of MDSC and the CD15⁺ MDSC fraction was added back either with the CD15⁻ PBMC or separated by Transwell® both at a 1:1 PBMC:MDSC ratio.

Cytokine analyses

Plasma was aliquoted and frozen at -80°C immediately during blood processing, then batch tested as per kit instructions using R&D systems 6-plex for GM-CSF, M-CSF, G-CSF, SCF, Flt-3 L, and CD14, 6-plex for IFN γ , IL-1 β , IL-6, IL-10, TNF α and VEGF and 1-plex for CRP.

Density separation method testing

Density separation media Ficoll-Paque PREMIUM (GE Healthcare), Polymorphprep™ (Axis-Shield) and Lympholyte®-poly (Cedarlane) were compared for activation and suppression of granulocytes.

Longitudinal MDSC kinetics in SIV-infection methods²

Specimen collection

Rhesus macaque (*Macaca mulatta*) blood and tissue were obtained from the Washington National Primate Research Center (WaNPRC). Animals were infected IV with SIV/DeltaB670. Pilot study blood draws were obtained 12 weeks post-SIV infection with no combination antiretroviral therapy (cART). Longitudinal study draws were obtained over the course of SIV infection including pre-SIV infection, post SIV infection, during cART, before and after therapeutic vaccination, before cART-cessation, and then every 10 weeks until study end at necropsy. Animals followed for MDSC kinetics were study control animals and received empty plasmid vector +/- LT adjuvant during a therapeutic vaccine protocol. cART regimen consisted of daily Viread (PMPA, 20 mg/kg), Emtriva (FTC, 50 mg/kg), and Isentress (Raltegravir, 100mg/kg). Blood was drawn into 10ml sodium heparin tubes, transferred to the Center of Infectious Disease Research (CIDR) at room temperature and processed immediately. Tissue was excised at necropsy, placed in 25ml RPMI, transferred to CIDR on wet ice and processed immediately.

Blood processing

Whole blood (100ul) was removed for cell counts, plasma was isolated for later cytokine analysis via centrifugation, and PBMC were obtained by density separation

² *Rationale behind modifications in protocol between human and animal experiments discussed in appendix A*

using Ficoll-Paque PREMIUM (GE Healthcare). Buffy coats were rinsed with PBS and resuspended in EasySep™ Buffer (Stemcell Technologies) for staining and MDSC isolation.

Staining

Whole blood counts utilized CountBright™ Absolute Counting Beads (Molecular Probes™) as per instructions using Cal-Lyse (Invitrogen™) and CD45 FITC (Becton Dickinson), CD66 PE (Miltenyi Biotec). Cells were stained for MDSC frequency using CD3 pacific blue (Becton Dickinson), CD11b PeCy7 (Miltenyi Biotec), CD14 APC (Becton Dickinson), CD16 PeCy5 (Becton Dickinson), CD66 PE (Miltenyi Biotec), HLA-DR APC-Cy7 (Fisher scientific). Cells were intracellularly stained (ICS) for *ex vivo* Ki67 activation with the following panel: CD8 PeCy7 (Biolegend), Ki67 Alexa Flour 488 (Becton Dickinson), CD3 APC (Becton Dickinson). Gating was determined by FMO and compensation control values.

MDSC isolation and PBMC co-cultures

CD66+ MDSC were separated from PBMC as per kit instructions using magnetic bead isolation (EasySep™) of PE-conjugated anti-CD66 (Miltenyi Biotec). CD66- PBMC were cultured at 37°C, 5% CO₂, overnight either alone or with CD66+ MDSC added back at a 1:1 ratio in custom arginine-low media: SILAC media (Sigma Aldrich) plus filter-sterilized L-arginine monohydrochloride (0.115mM, Sigma Aldrich) and filter-sterilized L-lysine hydrochloride (0.2186mM, Sigma Aldrich), 15% human serum (Sigma Aldrich), Penicillin-Streptomycin-Glutamine (0.5mg/ml, Thermo Fisher). Cells were then

stimulated with 1ug/ml 15mer SIVmac239 Gag peptide pool (NIH AIDS Reagent Program) or 0.4ug/ml Staphylococcal enterotoxin B from *Staphylococcus aureus* (Sigma Aldrich) for four days. Duplicate control un-stimulated wells for each cell mixture (PBMC alone, PBMC with CD66+MDSC) were included for background proliferation subtraction. Proliferation was measured by ICS for CD8 PeCy7 (Biolegend), Ki67 Alexa Flour 488 (Becton Dickinson), CD3 APC (Becton Dickinson). CD66+ MDSC-mediated suppression was measured by comparing the proliferation stimulated in the absence of CD66+ cells with the proliferation stimulated in the presence of CD66+ cells. Replicates were included for all PBMC wells, and PBMC + MDSC when MDSC yield allowed, and averaged.

Tissue processing at necropsy

Single-cell suspensions were made of ileum, spleen, and axillary, ileocecal, iliac, inguinal, mesenteric, cervical and retropharyngeal lymph nodes in 25ml RPMI, passed through a 100um filter and density separated with Ficoll. Buffy coats for each tissue were removed, rinsed with PBS, resuspended in EasySep™ Buffer (Stemcell Technologies) then stained for MDSC.

Plasma Cytokine Levels

Plasma was aliquoted and frozen at -80°C immediately during blood processing, then batch tested as per kit instructions using the Monkey Cytokine Magnetic 29-Plex Panel (ThermoFisher) for the following cytokines, chemokines and growth factors: GM-CSF, TNF- α , IL-1 β , IL-4, IL-6, MIG, VEGF, HGF, EGF, IL-8, IL-17, MIP-1 α , IL-

12, IL-10, FGF-Basic, IFN- γ , G-CSF, MCP-1, IL-15, IP-10, MIP-1 β , Eotaxin, RANTES, IL-1RA, I-TAC, MDC, IL-5, IL-2, and MIF.

Induction of MDSC via SIV viral products

Five day co-culture of uninfected rhesus macaque PBMC alone and with 1 μ g/ml SIV Gag peptide pool (NIH AIDS Reagent Program), heat killed (60°C 1 hour) or live SIV/DeltaB670 virus (provided by WaNPRC) were performed and analyzed for MDSC frequency at day 5 as done by Garg et al. [38].

Statistical Analyses

Data were prepared and analyzed using Prism 5 (Graphpad Software). Nonparametric tests were performed for MDSC frequency while parametric tests were utilized for cell suppression based on the population distribution of the data. Paired analyses were utilized when appropriate. Nonparametric tests employed were Mann-Whitney test for comparison of groups of unpaired data, Wilcoxon matched-pairs signed rank test for paired data and Spearman's rank-order correlation for X,Y correlation. Parametric tests employed were Student's unpaired T test for comparison of groups of unpaired data, Student's paired t test for comparison of groups of paired data and Pearson's correlation for X,Y correlation. A p value of <0.0017 was considered significant for cytokine associations to adjust for multiple comparisons, otherwise significance was identified at p<0.05 for univariate analyses. Multiple regression analysis with stepwise selection was performed by SAS.

Appendix A: Experimental optimization prior to longitudinal MDSC analyses

Experimental protocol was optimized between human MDSC characterization and longitudinal analyses of MDSC in the SIV-infected rhesus macaque. Changes included changing our culture set up from MDSC-containing vs. MDSC-depleted experiments to MDSC depleted + MDSC at a 1:1 ratio vs. MDSC depleted alone. This change was made for 2 reasons: 1) To obtain data on suppression over time on a per-cell level, reducing variables to the stage of infection alone, and 2) The criticism of our previous method was that there was no control included to take into account the effect of the magnetic depletion procedure on T cell proliferation. By comparing depleted PBMC +/- MDSC we were able to address both these concerns. Stimulation with peptide pools or polyclonal activators was added after 18hrs overnight culture of MDSC to control for two additional sources of variability: 1) Time of processing specimens, which was variable depending on how many specimens were obtained at a time, and 2) Time of MDSC and PBMC co-culture previous to stimulus, as this also varied based on the time of processing. By adding the overnight culture we also allowed the MDSC time to exert their suppressive effects. Furthermore, all experiments were performed in a low-arginine media. As we suspected arginase-1 may be responsible for the suppressive effects observed, using traditional media would have potentially masked the effect of arginase-1 as levels of arginine in RPMI would be difficult to overcome at 200mg/L compared to physiological levels of 12-19mg/L [102]. Lastly, we moved all functional experiments to a 96 well U-bottom plate utilizing the same layout and cell concentration at each time-point. This maximized the functional data we could obtain for each experiment by minimizing both

the cell number per experimental condition required (from 1×10^6 to 1.25×10^5) and downstream cell loss as ICS was performed and obtained on the HTS LSR2 system on the same plate. Plate edge effects caused by evaporation at edges were minimized by plating sterile PBS in all edge wells, then plating cells for culture in the 60 wells in the center.

Additionally, we tested our PBMC and MDSC separation methods to ensure suppression was not being induced by our separation methods. We compared the density separation media Ficoll-Paque PREMIUM (GE Healthcare) with Polymorphprep™ (Axis-Shield) and Lympholyte®-poly (Cedarlane). Each are endotoxin tested to reduce granulocyte activation, with Ficoll-Paque-PREMIUM having comparable maximum levels of endotoxin as Polymorphprep™ (<0.12 EU/ml vs. 0.13 EU/ml, respectively). We observed no difference in the activation or suppression of granulocytic cells isolated by each method. As we had much better discrimination of the PBMC layer with Ficoll-Paque, we chose to continue using this method of density separation. We performed a six day time-course with Ki67 to determine the ideal incubation time to encompass peptide and polyclonal responses, then compared CFSE and Ki67 for measurement of proliferation and suppression (data not shown). We observed no significant differences between the two with regards to suppression or measured response to stimuli, and proceeded with Ki67 at day 5 post-culture, day 4 post-stimulus as our proliferation marker going forward. The potential issues of using CFSE include cytotoxicity and additional manipulation of cells prior to culture, which is less desirable as it may decrease MDSC viability and observable suppression. With all of these procedural changes in

place we moved into an animal model with more confidence that the experimental variables had been minimized.

Acknowledgements

It takes a village to raise a graduate student. I am appreciative of every person who has helped me develop as an individual and as a scientist in the process of pursuing a Ph.D. I would like to thank the entire Horton lab, especially my mentor Helen for continuing to support this work even while nearly 5,000 miles away, and Ana, who is a wonderful teacher and guide. I would like to thank my committee: Dr. Helen Horton, Dr. Kevin Urdahl, Dr. Lisa Frenkel, Dr. Jenny Lund, Dr. Steve Polyak, and Dr. Corey Casper for their time, support and critique. I would like to especially thank my reading committee: Jenny, Kevin and Helen, for their helpful revisions and guidance. I would like to thank the U.W. Pathobiology graduate program for providing an inspiring and collaborative environment in which to conduct research. I would like to thank the NIH and Janssen for financial support of this work. Lastly, I would like to thank my family: my husband, Ian for helping me problem-solve, my parents, Harry and Karen for providing childcare at pivotal times, and my daughter Catherine for being understanding of the long days, and for sleeping through the night.

Vita

Sandra Dross was born in Syracuse, New York in 1980. She graduated from West Genesee Senior High School in 1998 and Rochester Institute of Technology in 2003 with a B.S. in Biotechnology. After two years of volunteer service in Americorps she joined the laboratory of Dr. Lisa Frenkel in 2005, studying the effectiveness of antiretroviral therapy and resulting drug resistance in HIV+ or at-risk women and infants. She joined the University of Washington Pathobiology Graduate Program in 2011 to pursue her Ph.D. Her graduate work in the laboratory of Dr. Helen Horton encompassed characterizing myeloid derived suppressor cells in a retroviral-infected host.

References

1. Gabrilovich, D.I., S. Ostrand-Rosenberg, and V. Bronte, *Coordinated regulation of myeloid cells by tumours*. Nat Rev Immunol, 2012. 12(4): p. 253-68.
2. Gabrilovich, D.I. and S. Nagaraj, *Myeloid-derived suppressor cells as regulators of the immune system*. Nat Rev Immunol, 2009. 9(3): p. 162-74.
3. Van Ginderachter, J.A., *The wound healing chronicles*. Blood, 2012. 120(3): p. 499-500.
4. Yang, L., et al., *Expansion of myeloid immune suppressor Gr⁺CD11b⁺ cells in tumor-bearing host directly promotes tumor angiogenesis*. Cancer Cell, 2004. 6(4): p. 409-21.
5. Talmadge, J.E. and D.I. Gabrilovich, *History of myeloid-derived suppressor cells*. Nat Rev Cancer, 2013. 13(10): p. 739-52.
6. Ostrand-Rosenberg, S., *Myeloid-derived suppressor cells: more mechanisms for inhibiting antitumor immunity*. Cancer Immunol Immunother, 2010. 59(10): p. 1593-600.
7. Murphy, K., et al., *Janeway's immunobiology*. 8th ed 2012, New York: Garland Science. xix, 868 p.
8. Rodriguez, P.C. and A.C. Ochoa, *Arginine regulation by myeloid derived suppressor cells and tolerance in cancer: mechanisms and therapeutic perspectives*. Immunol Rev, 2008. 222: p. 180-91.
9. Rodriguez, P.C., D.G. Quiceno, and A.C. Ochoa, *L-arginine availability regulates T-lymphocyte cell-cycle progression*. Blood, 2007. 109(4): p. 1568-73.
10. Munder, M., et al., *Arginase 1 is constitutively expressed in human granulocytes and participates in fungicidal activity*. Blood, 2005. 105(6): p. 2549-56.
11. Srivastava, M.K., et al., *Myeloid-derived suppressor cells inhibit T-cell activation by depleting cystine and cysteine*. Cancer Res, 2010. 70(1): p. 68-77.
12. Sakuishi, K., et al., *Emerging Tim-3 functions in antimicrobial and tumor immunity*. Trends Immunol, 2011. 32(8): p. 345-9.
13. Mahoney, K.M., G.J. Freeman, and D.F. McDermott, *The Next Immune-Checkpoint Inhibitors: PD-1/PD-L1 Blockade in Melanoma*. Clin Ther, 2015. 37(4): p. 764-82.
14. Noman, M.Z., et al., *PD-L1 is a novel direct target of HIF-1alpha, and its blockade under hypoxia enhanced MDSC-mediated T cell activation*. J Exp Med, 2014. 211(5): p. 781-90.
15. Talmadge, J.E., *Pathways mediating the expansion and immunosuppressive activity of myeloid-derived suppressor cells and their relevance to cancer therapy*. Clin Cancer Res, 2007. 13(18 Pt 1): p. 5243-8.
16. Reglier, H., et al., *Lack of IL-10 and IL-13 production by human polymorphonuclear neutrophils*. Cytokine, 1998. 10(3): p. 192-8.

17. De Santo, C., et al., *Invariant NKT cells modulate the suppressive activity of IL-10-secreting neutrophils differentiated with serum amyloid A*. Nat Immunol, 2010. 11(11): p. 1039-46.
18. Whicher, J.T., et al., *Acute phase response of serum amyloid A protein and C reactive protein to the common cold and influenza*. J Clin Pathol, 1985. 38(3): p. 312-6.
19. Husebekk, A., H. Permin, and G. Husby, *Serum amyloid protein A (SAA): an indicator of inflammation in AIDS and AIDS-related complex (ARC)*. Scand J Infect Dis, 1986. 18(5): p. 389-94.
20. Shainkin-Kestenbaum, R., et al., *Serum amyloid A (SAA) in viral infection: rubella, measles and subacute sclerosing panencephalitis (SSPE)*. Clin Exp Immunol, 1982. 50(3): p. 503-6.
21. Sarov, I., et al., *Serum amyloid A levels in patients with infections due to cytomegalovirus, varicella-zoster virus, and herpes simplex virus*. J Infect Dis, 1982. 146(3): p. 443.
22. Kramer, H.B., et al., *Elevation of intact and proteolytic fragments of acute phase proteins constitutes the earliest systemic antiviral response in HIV-1 infection*. PLoS Pathog, 2010. 6(5): p. e1000893.
23. Fuster, D., et al., *Inflammatory cytokines and mortality in a cohort of HIV-infected adults with alcohol problems*. AIDS, 2014. 28(7): p. 1059-64.
24. Hijmans, W. and J.D. Sipe, *Levels of the serum amyloid A protein (SAA) in normal persons of different age groups*. Clin Exp Immunol, 1979. 35(1): p. 96-100.
25. Ballou, S.P., et al., *Quantitative and qualitative alterations of acute-phase proteins in healthy elderly persons*. Age Ageing, 1996. 25(3): p. 224-30.
26. Goh, C., S. Narayanan, and Y.S. Hahn, *Myeloid-derived suppressor cells: the dark knight or the joker in viral infections?* Immunol Rev, 2013. 255(1): p. 210-21.
27. Chen, S., et al., *Immunosuppressive functions of hepatic myeloid-derived suppressor cells of normal mice and in a murine model of chronic hepatitis B virus*. Clin Exp Immunol, 2011. 166(1): p. 134-42.
28. Norris, B.A., et al., *Chronic but not acute virus infection induces sustained expansion of myeloid suppressor cell numbers that inhibit viral-specific T cell immunity*. Immunity, 2013. 38(2): p. 309-21.
29. Huang, A., et al., *Myeloid-derived suppressor cells regulate immune response in patients with chronic hepatitis B virus infection through PD-1-induced IL-10*. J Immunol, 2014. 193(11): p. 5461-9.
30. Liu, Y., et al., *Expansion of myeloid-derived suppressor cells from peripheral blood decreases after 4-week antiviral treatment in patients with chronic hepatitis C*. Int J Clin Exp Med, 2014. 7(4): p. 998-1004.
31. Zeng, Q.L., et al., *Myeloid-derived suppressor cells are associated with viral persistence and downregulation of TCR zeta chain expression on CD8(+) T cells in chronic hepatitis C patients*. Mol Cells, 2014. 37(1): p. 66-73.
32. Nonnenmann, J., et al., *Lack of significant elevation of myeloid-derived suppressor cells in peripheral blood of chronically hepatitis C virus-infected individuals*. J Virol, 2014. 88(13): p. 7678-82.

33. Grutzner, E., et al., *Kinetics of human myeloid-derived suppressor cells after blood draw*. J Transl Med, 2016. 14: p. 2.
34. Trellakis, S., et al., *Granulocytic myeloid-derived suppressor cells are cryosensitive and their frequency does not correlate with serum concentrations of colony-stimulating factors in head and neck cancer*. Innate Immun, 2013. 19(3): p. 328-36.
35. Vollbrecht, T., et al., *Chronic progressive HIV-1 infection is associated with elevated levels of myeloid-derived suppressor cells*. AIDS, 2012. 26(12): p. F31-7.
36. Bowers, N.L., et al., *Immune suppression by neutrophils in HIV-1 infection: role of PD-L1/PD-1 pathway*. PLoS Pathog, 2014. 10(3): p. e1003993.
37. Qin, A., et al., *Expansion of monocytic myeloid-derived suppressor cells dampens T cell function in HIV-1-seropositive individuals*. J Virol, 2013. 87(3): p. 1477-90.
38. Garg, A. and S.A. Spector, *HIV type 1 gp120-induced expansion of myeloid derived suppressor cells is dependent on interleukin 6 and suppresses immunity*. J Infect Dis, 2014. 209(3): p. 441-51.
39. Tumino, N., et al., *In HIV-positive patients, myeloid-derived suppressor cells induce T-cell anergy by suppressing CD3zeta expression through ELF-1 inhibition*. AIDS, 2015. 29(18): p. 2397-407.
40. Wang, L., et al., *Expansion of myeloid-derived suppressor cells promotes differentiation of regulatory T cells in HIV-1+ individuals*. AIDS, 2016.
41. Gama, L., et al., *Expansion of a subset of CD14^{high}CD16^{neg}CCR2^{low}/neg monocytes functionally similar to myeloid-derived suppressor cells during SIV and HIV infection*. J Leukoc Biol, 2012. 91(5): p. 803-16.
42. Sui, Y., et al., *Vaccine-induced myeloid cell population dampens protective immunity to SIV*. J Clin Invest, 2014. 124(6): p. 2538-49.
43. Schmitz, J.E., et al., *Control of viremia in simian immunodeficiency virus infection by CD8⁺ lymphocytes*. Science, 1999. 283(5403): p. 857-60.
44. Ndhlovu, Z.M., et al., *High-dimensional immunomonitoring models of HIV-1-specific CD8 T-cell responses accurately identify subjects achieving spontaneous viral control*. Blood, 2013. 121(5): p. 801-11.
45. Brenchley, J.M., et al., *Microbial translocation is a cause of systemic immune activation in chronic HIV infection*. Nat Med, 2006. 12(12): p. 1365-71.
46. Younas, M., et al., *Immune activation in the course of HIV-1 infection: Causes, phenotypes and persistence under therapy*. HIV Med, 2016. 17(2): p. 89-105.
47. Giorgi, J.V., et al., *Shorter survival in advanced human immunodeficiency virus type 1 infection is more closely associated with T lymphocyte activation than with plasma virus burden or virus chemokine coreceptor usage*. J Infect Dis, 1999. 179(4): p. 859-70.
48. Althoff, K.N., et al., *Comparison of risk and age at diagnosis of myocardial infarction, end-stage renal disease, and non-AIDS-defining cancer in HIV-infected versus uninfected adults*. Clin Infect Dis, 2015. 60(4): p. 627-38.

49. Verschoor, C.P., et al., *Blood CD33(+)HLA-DR(-) myeloid-derived suppressor cells are increased with age and a history of cancer*. J Leukoc Biol, 2013. 93(4): p. 633-7.
50. Cahill, S. and R. Valadez, *Growing older with HIV/AIDS: new public health challenges*. Am J Public Health, 2013. 103(3): p. e7-e15.
51. Holtzer, R., R.A. Zweig, and L.J. Siegel, *Learning From The Past and Planning For The Future: The Challenges Of And Solutions For Integrating Aging Into Doctoral Psychology Training*. Train Educ Prof Psychol, 2012. 6(3): p. 142-150.
52. *World Health Organization launches new initiative to address the health needs of a rapidly ageing population*. Cent Eur J Public Health, 2004. 12(4): p. 210, 216.
53. Nguyen, N. and M. Holodniy, *HIV infection in the elderly*. Clin Interv Aging, 2008. 3(3): p. 453-72.
54. Samji, H., et al., *Closing the gap: increases in life expectancy among treated HIV-positive individuals in the United States and Canada*. PLoS One, 2013. 8(12): p. e81355.
55. Venkatesh, K.K., K.H. Mayer, and C.C. Carpenter, *Low-cost generic drugs under the President's Emergency Plan for AIDS Relief drove down treatment cost; more are needed*. Health Aff (Millwood), 2012. 31(7): p. 1429-38.
56. Goronzy, J.J., et al., *Value of immunological markers in predicting responsiveness to influenza vaccination in elderly individuals*. J Virol, 2001. 75(24): p. 12182-7.
57. Rosenberg, C., et al., *Age is an important determinant in humoral and T cell responses to immunization with hepatitis B surface antigen*. Hum Vaccin Immunother, 2013. 9(7): p. 1466-76.
58. Kroon, F.P., et al., *Antibody response to influenza, tetanus and pneumococcal vaccines in HIV-seropositive individuals in relation to the number of CD4+ lymphocytes*. AIDS, 1994. 8(4): p. 469-76.
59. Gavazzi, G. and K.H. Krause, *Ageing and infection*. Lancet Infect Dis, 2002. 2(11): p. 659-66.
60. Yager, E.J., et al., *Age-associated decline in T cell repertoire diversity leads to holes in the repertoire and impaired immunity to influenza virus*. J Exp Med, 2008. 205(3): p. 711-23.
61. Arnold, C.R., et al., *Gain and loss of T cell subsets in old age--age-related reshaping of the T cell repertoire*. J Clin Immunol, 2011. 31(2): p. 137-46.
62. Naylor, K., et al., *The influence of age on T cell generation and TCR diversity*. J Immunol, 2005. 174(11): p. 7446-52.
63. Boehm, T. and J.B. Swann, *Thymus involution and regeneration: two sides of the same coin?* Nat Rev Immunol, 2013. 13(11): p. 831-8.
64. Hakim, F.T., et al., *Age-dependent incidence, time course, and consequences of thymic renewal in adults*. J Clin Invest, 2005. 115(4): p. 930-9.
65. Goronzy, J.J. and C.M. Weyand, *T cell development and receptor diversity during aging*. Curr Opin Immunol, 2005. 17(5): p. 468-75.
66. Aw, D. and D.B. Palmer, *The origin and implication of thymic involution*. Aging Dis, 2011. 2(5): p. 437-43.

67. Cicin-Sain, L., et al., *Dramatic increase in naive T cell turnover is linked to loss of naive T cells from old primates*. Proc Natl Acad Sci U S A, 2007. 104(50): p. 19960-5.
68. Appay, V., et al., *Accelerated immune senescence and HIV-1 infection*. Exp Gerontol, 2007. 42(5): p. 432-7.
69. Desai, S. and A. Landay, *Early immune senescence in HIV disease*. Curr HIV/AIDS Rep, 2010. 7(1): p. 4-10.
70. Cutrell, J. and R. Bedimo, *Non-AIDS-defining cancers among HIV-infected patients*. Curr HIV/AIDS Rep, 2013. 10(3): p. 207-16.
71. Franceschi, C., *Inflammaging as a major characteristic of old people: can it be prevented or cured?* Nutr Rev, 2007. 65(12 Pt 2): p. S173-6.
72. Deeks, S.G., R. Tracy, and D.C. Douek, *Systemic effects of inflammation on health during chronic HIV infection*. Immunity, 2013. 39(4): p. 633-45.
73. Thompson, W.W., et al., *Influenza-associated hospitalizations in the United States*. JAMA, 2004. 292(11): p. 1333-40.
74. Thompson, W.W., et al., *Mortality associated with influenza and respiratory syncytial virus in the United States*. JAMA, 2003. 289(2): p. 179-86.
75. McKittrick, N., et al., *Improved immunogenicity with high-dose seasonal influenza vaccine in HIV-infected persons: a single-center, parallel, randomized trial*. Ann Intern Med, 2013. 158(1): p. 19-26.
76. Heithoff, D.M., et al., *Conditions that diminish myeloid-derived suppressor cell activities stimulate cross-protective immunity*. Infect Immun, 2008. 76(11): p. 5191-9.
77. Poschke, I., et al., *Immature immunosuppressive CD14+HLA-DR-/low cells in melanoma patients are Stat3hi and overexpress CD80, CD83, and DC-sign*. Cancer Res, 2010. 70(11): p. 4335-45.
78. Sauter, D. and F. Kirchhoff, *HIV replication: a game of hide and sense*. Curr Opin HIV AIDS, 2016. 11(2): p. 173-81.
79. O'Neill, L.A., D. Golenbock, and A.G. Bowie, *The history of Toll-like receptors - redefining innate immunity*. Nat Rev Immunol, 2013. 13(6): p. 453-60.
80. Sandler, N.G. and D.C. Douek, *Microbial translocation in HIV infection: causes, consequences and treatment opportunities*. Nat Rev Microbiol, 2012. 10(9): p. 655-66.
81. Okwan-Duodu, D., et al., *Obesity-driven inflammation and cancer risk: role of myeloid derived suppressor cells and alternately activated macrophages*. Am J Cancer Res, 2013. 3(1): p. 21-33.
82. Zhang, H. and G.G. Meadows, *Chronic alcohol consumption enhances myeloid-derived suppressor cells in B16BL6 melanoma-bearing mice*. Cancer Immunol Immunother, 2010. 59(8): p. 1151-9.
83. Ortiz, M.L., et al., *Myeloid-derived suppressor cells in the development of lung cancer*. Cancer Immunol Res, 2014. 2(1): p. 50-8.
84. Hegde, V.L., M. Nagarkatti, and P.S. Nagarkatti, *Cannabinoid receptor activation leads to massive mobilization of myeloid-derived suppressor cells with potent immunosuppressive properties*. Eur J Immunol, 2010. 40(12): p. 3358-71.

85. Rahmanian, S., et al., *Cigarette smoking in the HIV-infected population*. Proc Am Thorac Soc, 2011. 8(3): p. 313-9.
86. Petry, N.M., *Alcohol use in HIV patients: what we don't know may hurt us*. Int J STD AIDS, 1999. 10(9): p. 561-70.
87. Crum-Cianflone, N., et al., *Obesity among patients with HIV: the latest epidemic*. AIDS Patient Care STDS, 2008. 22(12): p. 925-30.
88. Kumar, V., et al., *The Nature of Myeloid-Derived Suppressor Cells in the Tumor Microenvironment*. Trends Immunol, 2016.
89. Wolpe, S.D., et al., *Macrophages secrete a novel heparin-binding protein with inflammatory and neutrophil chemokinetic properties*. J Exp Med, 1988. 167(2): p. 570-81.
90. Simpson, K.D., D.J. Templeton, and J.V. Cross, *Macrophage migration inhibitory factor promotes tumor growth and metastasis by inducing myeloid-derived suppressor cells in the tumor microenvironment*. J Immunol, 2012. 189(12): p. 5533-40.
91. Waigel, S., et al., *MIF inhibition reverts the gene expression profile of human melanoma cell line-induced MDSCs to normal monocytes*. Genom Data, 2016. 7: p. 240-2.
92. Zhao, X., et al., *TNF signaling drives myeloid-derived suppressor cell accumulation*. J Clin Invest, 2012. 122(11): p. 4094-104.
93. Santos-Oliveira, J.R., et al., *Microbial translocation induces an intense proinflammatory response in patients with visceral leishmaniasis and HIV type 1 coinfection*. J Infect Dis, 2013. 208(1): p. 57-66.
94. Calandra, T. and T. Roger, *Macrophage migration inhibitory factor: a regulator of innate immunity*. Nat Rev Immunol, 2003. 3(10): p. 791-800.
95. Nazli, A., et al., *Exposure to HIV-1 directly impairs mucosal epithelial barrier integrity allowing microbial translocation*. PLoS Pathog, 2010. 6(4): p. e1000852.
96. Youn, J.I., et al., *Subsets of myeloid-derived suppressor cells in tumor-bearing mice*. J Immunol, 2008. 181(8): p. 5791-802.
97. Movahedi, K., et al., *Identification of discrete tumor-induced myeloid-derived suppressor cell subpopulations with distinct T cell-suppressive activity*. Blood, 2008. 111(8): p. 4233-44.
98. Pan, T., et al., *17beta-estradiol enhances the expansion and activation of myeloid-derived suppressor cells via STAT3 signaling in human pregnancy*. Clin Exp Immunol, 2016.
99. Gervassi, A., et al., *Myeloid derived suppressor cells are present at high frequency in neonates and suppress in vitro T cell responses*. PLoS One, 2014. 9(9): p. e107816.
100. Addo, M.M. and M. Altfeld, *Sex-based differences in HIV type 1 pathogenesis*. J Infect Dis, 2014. 209 Suppl 3: p. S86-92.
101. *Guidelines for the use of antiretroviral agents in HIV-1-infected adults and adolescents.*, in Department of Health and Human Services., P.o.A.G.f.A.a. Adolescents, Editor 2016: Available at <http://www.aidsinfo.nih.gov/ContentFiles/AdultandAdolescentGL.pdf>.

102. Brigham, M.P., W.H. Stein, and S. Moore, *The Concentrations of Cysteine and Cystine in Human Blood Plasma*. J Clin Invest, 1960. 39(11): p. 1633-8.